ANALYSIS OF TOTAL OZONE DATA FROM REYKJAVÍK FOR THE PERIOD 1957–1991

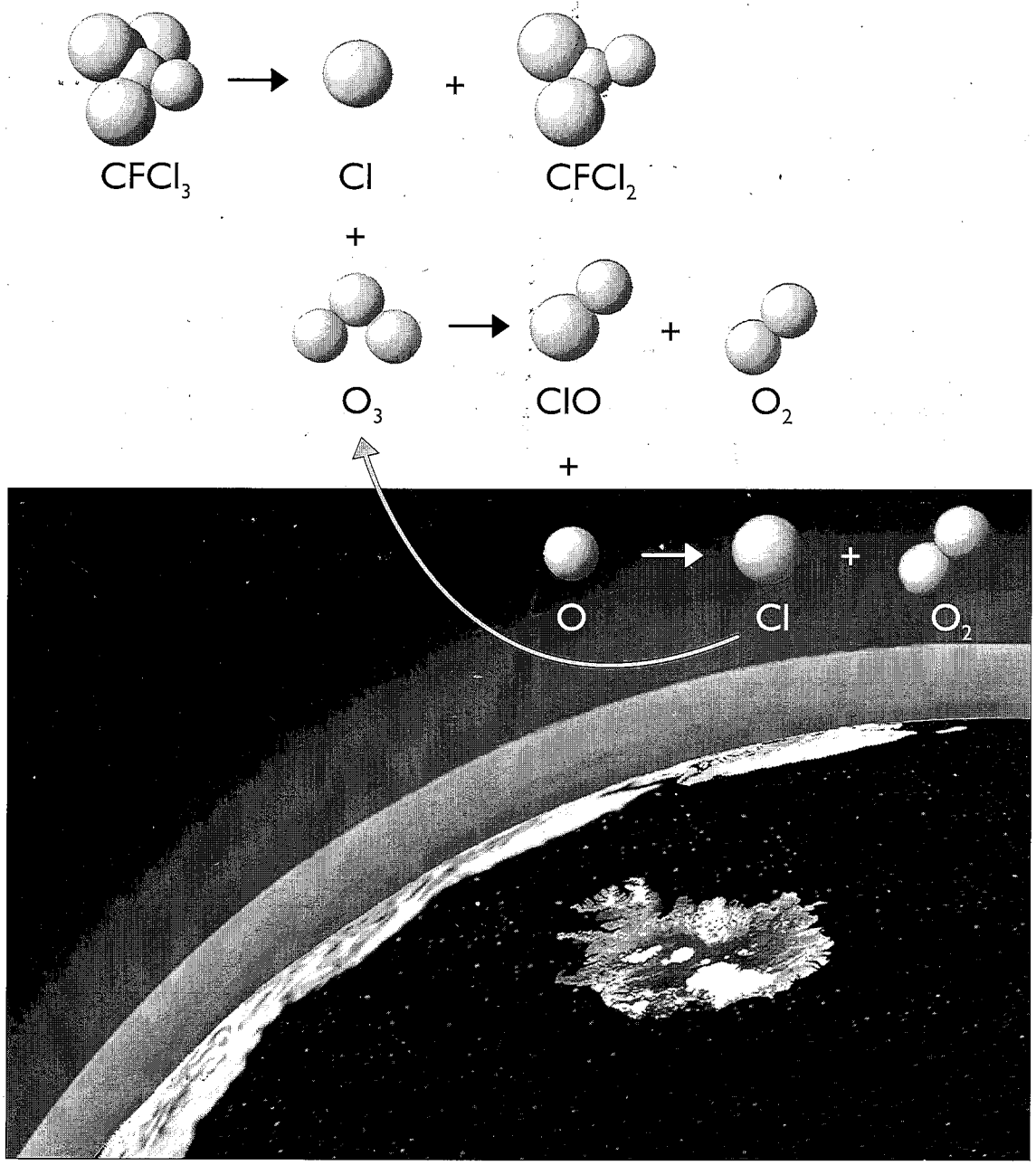

Science Institute, University of Iceland

ANALYSIS OF TOTAL OZONE DATA FROM REYKJAVIK FOR THE PERIOD 1957–1991

RH92–3

Gudmundur G. Bjarnason, Örnólfur E. Rögnvaldsson, Thorsteinn I. Sigfússon, Thor Jakobsson, Bardi Thorkelsson:
Analysis of Total Ozone Data from Reykjavik for the Period 1957–1991
Science Institute, University of Iceland, April 1992, report RH92–3.
Cover by Bjarni Thor Júliusson.

Analysis of Total Ozone Data from Reykjavik for the Period 1957–1991

Gudmundur G. Bjarnason[1], Örnólfur E. Rögnvaldsson[1],
Thorsteinn I. Sigfússon[1], Thor Jakobsson[2],
Bardi Thorkelsson[2]

[1]Science Institute, University of Iceland,
Dunhagi 3, IS-107 Reykjavik, Iceland.
Tel. +354-1-694800, fax +354-1-28911

[2]Icelandic Meteorological Office,
Bústadavegur 9, IS-150 Reykjavik, Iceland.
Tel. +354-1-600600, fax +354-1-28121

Abstract

Total ozone measurements using a Dobson spectrophotometer have been performed on a regular basis at Reykjavik (64°08′N, 21°54′W), Iceland, since 1957. The data set for the entire period of observations has been critically examined. Due to problems related to the calibration of the instrument the data record of ozone observations are divided into two periods in the following analysis (1957 to 1977 and 1977 to 1990). A statistical model was developed to fit the data and estimate long term changes in total ozone. The model includes seasonal variations, solar cycle influences, Quasi-Biennial-Oscillation (QBO) effects and linear trends. Some variants of the model are applied to investigate to what extent the estimated trends depend on the form of the model. Trend analysis of the revised data reveals a statistically significant linear decrease of $0.11 \pm 0.07\%$ per year in the annual total ozone amount during the earlier period and $0.30 \pm 0.11\%$ during the latter. The annual total ozone decline since 1977 is caused by a $0.47 \pm 0.14\%$ decrease per year during the summer with no significant change during the winter or fall. The effect of the 11.2 year solar cycle is particularly strong in the data during the early months of the year and in the westerly phase of the QBO. A correlation coefficient of 0.73 is calculated for the total ozone amount and the sunspot number in February when ozone changes by about 25% over one solar cycle. On an annual basis ozone varies by $3.5 \pm 0.8\%$ over a solar cycle and by $2.1 \pm 0.6\%$ over a QBO for the whole observation period. Comparisons of the total ozone data made at Reykjavik during the last 13 years with total ozone as measured by the Total Ozone Mapping Spectrometer (TOMS) on the Nimbus 7 satellite show an excellent agreement for solar zenith angles less than 80 degrees at times of satellite overpass. Comparisons with results of the zonally averaged TOMS data at this latitude suggest that the stratospheric ozone decrease at other longitudes during the winter may contribute to the observed summer decline of total ozone above Iceland.

1 Introduction

Natural variations of the total ozone concentration in a vertical column from the surface through the entire atmosphere have long been known to exist. This includes the seasonal variations, solar cycle effects and influences related to changes of the stratospheric circulation patterns. Detection of linear trends over long time periods is difficult because of the relatively large variability of these natural fluctuations. Increased efforts in analyzing records of total ozone measurements have been made in recent years. This is related to the discovery of a drastical decline of stratospheric ozone levels in the Antarctic [Farman *et al.*, 1985] and the recent indications of potential loss of total ozone in the northern hemisphere [Hofmann and Deshler, 1991; Koike *et al.*, 1991]. Prompted in part by the discovery of the accelerated ozone decline in the Antarctic (the 'ozone hole'), theories have rapidly advanced in the attempt to explain the phenomenon. This effort has greatly enriched our knowledge and understanding of the physical processes taking place in the middle atmosphere [see, e.g. Solomon, 1990]. It is concluded that the remarkable ozone changes are related to heterogeneous chemical reactions occurring on the surfaces of particles in polar stratospheric clouds (PSCs), releasing highly reactive chlorine species from relatively inactive compounds (e.g. HCl, $ClONO_2$). The elevated levels of Cl radicals would then enhance the proposed gas-phase chlorine-catalyzed ozone destructive cycles. [Solomon *et al.*, 1986; McElroy *et al.*, 1986; Anderson *et al.*, 1991]. PSCs are also considered to be important in removing odd nitrogen ($NO + NO_2$) from the lower stratosphere (denitrification) which would otherwise be able to avert ozone destruction by converting reactive chlorine (ClO) to an inactive form ($ClONO_2$). The formation of PSCs depends strongly on the ambient temperature and therefore on the dynamical state of the atmosphere in this region [Hanson and Mauersberger, 1988; Fiocco *et al.*, 1991]. The cold temperatures necessary for their formation are frequent in the Antarctic where the winter polar vortex is relatively large and isolated for extended periods of time [McCormick *et al.*, 1982; Hamill *et al.*, 1986; Crutzen and Arnold, 1987].

Northern hemispheric temperatures in the lower stratosphere are generally 10-15°K higher than temperatures in the Antarctic at the same altitude and corresponding season. This is a consequence of a smaller sized polar vortex and more pronounced wave activity, including the efficient mixing of warm air at lower latitudes with the colder polar air. Accordingly, the number of PSCs in the Arctic is less than 10% of the number observed in the Antarctic [McCormick *et al.*, 1982] and may not last long enough to significantly denitrify the lower stratospheric region or allowing for the full completion of the ozone-damaging chemical processes. Therefore, the interhemispheric differences in climatological conditions are believed to be the main reason for the relatively slower rate of ozone decline in the Arctic. The effective chemical destruction processes related to the elevated chlorine levels of human origin are, however, common to both regions. Evidence from high altitude aircraft missons to the Arctic (AASE, Airborne Arctic Stratospheric Expedition) [Turco *et*

al., 1990] during the winter 1988–1989 has shown large abundances of ClO mixing ratios, exceeding 1 ppbv (parts per billion by volume) [Brune *et al.*, 1990], which along with BrO, OH and O species are capable of perturbing large portions of the ozone layer in the north polar region, comparable to those observed in Antarctica. Although some evidence of heterogeneous processes were found no clear depletion of polar total ozone were observed because of a highly perturbed arctic vortex resulting from a major stratospheric warming occurring in early March [Newman *et al.*, 1990]. Similar conclusions are also drawn from the CHEOPS (CHEmistry of Ozone in the Polar Stratosphere) research campaign during the arctic winter 1989–1990 [Pommereau and Schmidt, 1991]. (Measurements of the Upper Atmosphere Research Satellite (UARS) indicate ClO levels exceeding 1.2 ppbv in January 1992, confirmed by the second Airborne Arctic Stratospheric Expedition (AASE II) observing mixing ratios up to 1.5 ppbv at ER-2 flight altitudes.)

An important contribution to the verification of the validity of current theories of observed ozone decline in both hemispheres is a critical evaluation of the existing records of the history of total ozone changes at various ground-based Dobson stations. Intercomparisons with available satellite data, which have become increasingly reliable in recent years, provide a useful test for possible inconsistencies in the records.

Both the satellite and ground-based Dobson measurements [Stolarski *et al.*, 1991; Bojkov *et al.*, 1990] show that trends in total ozone are largest at the highest latitudes, particulaly during the early spring. Assessment of long term changes in stratospheric ozone at high latitudes must be based on records of data extending over many years or even decades. This is particularly true during the winter season, showing large interannual variability of ozone associated with sudden stratospheric warmings, the influences of the tropical Quasi-Biennial-Oscillation (QBO) and the substantial role of the 11.2 year solar cycle in shaping the long term course of total ozone amount. Further, measurements made during the winter at large solar zenith angles are systematically erroneous and less reliable relative to the rest of the year.

As for other Dobson stations, most of the observational results from the Dobson ozone site in Reykjavik, operated by the Icelandic Meteorological Office, have been concurrently reported to the World Ozone Data Centre (WO_3DC) of the World Meteorological Organization (WMO) operated by the Atmospheric Environment Service (AES) in Toronto, Canada. Total ozone data for all the Dobson stations are made available by the same organization and have been used in several previous trend studies with various degrees of averaging and revisions [WMO, 1990]. However, the data from Reykjavik have been excluded in some studies [Bojkov *et al.*, 1990] because of incompatibility with trends appearing in the data of other stations. We have found that the anomalous linear trends are due to problems related to the calibration of the instrument in 1977. Comparison studies with satellite data [Barthia *et al.*, 1984; Bojkov *et al.*, 1988; Hesse, 1992; Bojkov, personal communications], including this work, show that the relative precision of total ozone as measured at Reykjavik is among the highest of all Dobson stations. Only a few

ground-based long term ozone measurements are available for the northern polar region [Bojkov, 1988]. On the basis of the high precision apparent in the data relative to the satellite data and the long existing record available from Reykjavik, this is possibly the only station that is suitable for use in long-term trend analysis, including solar cycle and human influences, in this part of the hemisphere.

This paper is organized as follows: Section 2 briefly describes the reevaluation of the data and difficulties related to the calibration of the instrument. In section 3 we describe the statistical model, different variants of the model and assumptions made when performing the calculations. Section 4 presents the model results for the long term trends, both linear and of solar origin, along with comparisons with available measurements by the Total Ozone Mapping Spectrometer (TOMS) on the Nimbus 7 satellite. Section 5 summarizes the results of the study.

2 Revisions of the data set

In this paper we present results based on coordinated data. After a careful examination of the daily records of each measurement for the entire observing period it was found necessary to apply several corrections and revisions to the data set, especially for the period 1957 to 1977. During this period some badly performed measurements had to be excluded from the data set while a few others previously rejected could be added by examining the daily log register on each measurement. Some typographical errors could also be identified. A thorough comparison of results from measurements using the CC′ wavelength pairs (311.5nm, 332.4nm; 332.4nm, 453.6nm) and the AD wavelength pairs (305.5nm, 325.4nm; 317.6nm, 339.8nm) on direct sun (ADDS) shows that the previously published data for the CC′ measurements underestimate the total ozone amount. This discrepancy is mainly due to the use of erroneous cloud correction tables for this observing station during the period 1957 to 1977. A new relationship between the ADDS and CC′ measurements was established and used for this time period. This leads to a general change of about 0.5–2.5% in most of the total ozone values. Measurements at the C wavelength pair during both time periods and the CD wavelength pairs (zenith blue, ZB, or cloudy, ZC) during the latter period are made at large solar zenith angles when direct sun observations are impossible to perform and CC′ observations give very inaccurate results. From early November to early February solar zenith angles always exceed 80° at this latitude. Measurements made during mid-winter thus have a low reliability. The data from 1977 to the present did not have to be treated as rigorously because of the higher quality in the measurements and the original data reduction. Only minor corrections had to be made for the years 1977 to 1982. The data after 1982 used in this work is almost identical to the data as published by the AES.

The Dobson instrument (spectrophotometer no. 50) situated at Reykjavik has been calibrated twice relative to a standard since operation began in 1957. An intercomparison carried out in Boulder, CO, USA, (primary standard, Dobson no.

83) in 1977 showed that when measuring at the AD wavelengths the total ozone values were 7–8% too low relative to the standard. However, the comparisons made were very limited and hardly useful since the instrument was in a bad shape after the shipping to Boulder (Komhyr, personal communications). Hence, no definite conclusions can be drawn from this intercomparison. Another calibration at Arosa, Switzerland in 1990 resulted in 3.2% lower values than the secondary standard no. 65 at the AD wavelengths. Comparison with the TOMS data (version 6) indicates no significant relative drift in the Dobson instrument during the period 1979–1991 and hence no attempt has been made to correct the original data for the drift suggested by the intercomparison in 1990.

A different observation series applied in this study were the temperature measurements obtained from a meteorological upper air radiosonde station at Keflavik Airport, approximately 50km away from Reykjavik. The balloon measurements are performed twice daily by the Icelandic Meteorological Office. The processed temperature data were obtained from the climate data bank at the Naval Oceanography Command Detachment in Asheville, NC, USA. Based on the generally high and well established correlation of total ozone with lower stratospheric temperatures, inconsistencies in the ozone record can sometimes be identified after an intercomparison with the temperatures at the 100mb pressure level. After completion of the revisions on the total ozone data set, as described above, and comparison of the entire data set with the 100mb temperatures, only a few individual measurements had to be rejected and excluded from the data set. In Figure 1 we show the published total ozone data at Reykjavik in the year 1986 along with the temperature record at the 100mb pressure level. The close temperature-ozone relation for time scales of the order of days is evident and the major warming during mid-February is well reproduced in the ozone data. As originally suggested by Dobson [1968] the short term variations are due to ozone transport in cyclones and anti-cyclones propagating into the lower stratosphere. The occasional low values of total ozone, related to tropospheric anti-cyclonic disturbances, have been referred to as 'mini-holes' in recent years [Newman *et al.*, 1988]. Mini-hole events on the edge of the vortex only partially represent the behavior of total ozone in the polar north as suggested by a recent model study by Rood *et al.* [1992].

Although the revised data set is of a higher quality now, the functional form of ozone trends resulting from our trend analysis model do not change significantly when using the originally published data provided that data are properly selected from different calibration periods.

3 Modeling of the data

In this study a statistical model was developed and used to estimate long term changes of the revised total ozone data. Natural variations have to be accounted for in the model when linear trends in total ozone are determined. These include

solar cycle signals, QBO related influences and seasonal variations. The seasonal variation was accounted for in the trend model by including a superposition of six (or four) harmonics (12, 6, 4 etc. months) plus an annual average ozone amount. Having removed the natural effects, one can presumably deduce linear trends from the residuals. The general form of the model for a time series of ozone can be presented as follows:

$$O_3(t) = (\text{seasonal variations}) + (\text{linear trends}) + \gamma \text{QBO}(t) + \delta \text{SOL}(t) + e(t). \quad (1)$$

The parameters γ and δ are the amplitudes of the QBO and solar cycle influences in total ozone as determined by the model. The amplitudes and phases of the QBO are based on data of monthly means of the zonal winds at the 50mb pressure level as measured at Canton Island (2°46′S, 171°43′W), Maldives (0°41′S, 73°09′E) and Singapore (1°22′N, 103°55′E). The data were made available by the Freie Universität Berlin through the National Center for Atmospheric Research (NCAR), Boulder, CO, USA. The data from Canton Island is for the period 1953–1967, the Maldives data covers 1967–1975 and the Singapore data 1976–1991. The entire QBO time series is shown in Figure 2. The effect of solar variability (variable SOL(t) in equation (1)), is modeled with a linear dependence on either the monthly mean sunspot numbers as published by the National Geophysical Data Center, Boulder, CO, USA, or the 10.7cm solar flux ($F_{10.7}$) data from the World Data Centre in Ottawa, Canada. The two time series (Figure 3) are the most commonly used indices of solar activity, including UV-flux variability.

At the outset we assume that the errors $e(t)$ are normally (Gaussian) distributed and independent. The method of generalized least squares is used where each measurement is weighted according to its estimated standard deviation depending on the wavelength pair used [Basher, 1982]. The standard deviations used are 3% for ADDS measurements, 5% for CDDS measurements and 6% for all other measurements. This causes the higher errors to be more biased towards the winter season since the C and CD measurements are most common for solar zenith angles greater than 80°. The weight-matrix in the model then has diagonal elements $w_{ii} = 1/\sigma^2$ while all the other elements are 0 (see the Appendix). The error term in equation (1) showed an autoregressive structure when the model was fitted to the data. This is evident in Figure 4, which shows $e(t_i)$ as a function of $e(t_{i-1})$ whenever observations are made on at least two consecutive days. The correlation coefficient between the two residuals is 0.65. This suggests that a more comprehensive model is needed since estimated standard errors in the model parameters are dependent on how autoregression is treated (see e.g. Seber and Wild, 1989, pp. 21–89 and 271–286). The simplest model which takes this structure into account is the AR(1) model

$$e(t_i) = \phi e(t_{i-1}) + a(t_i) \quad (2)$$

where the $a(t_i)$'s are assumed to be uncorrelated random variables with zero mean and $e(t_1) = a(t_1)$. ϕ is the AR-parameter to be determined from the data like the

other model parameters. Equation (2) for the errors is restricted to a time series with a constant sampling frequency.

The natural extension to series with unequally spaced data is

$$e(t_i) = \phi^{\Delta t} e(t_{i-1}) + a(t_i) \tag{3}$$

where $\Delta t = |t_i - t_{i-1}|$ is the length of the time interval between two consecutive measurements. Including an AR(1) structure in modeling of unequally spaced data complicates calculations of the weigth-matrix in the least squares method and some computational problems arise when determining ϕ (or any other parameters of the error model, if it is more complicated). This problem could be solved by applying a 'filling' procedure to substitute for the missing data in the record. This could, however, seriously influence the deduced model parameters and increase the estimated standard errors due to the additionally imposed AR-structure to the data, depending on the procedure used.

There are two significant sources of correlation between consecutive errors both of which suggest that including an AR structure in the model is not justified. One is inherent in the model itself and the other is related to short natural time scales for total ozone changes (i.e. a few days). The model is not able to realistically simulate rapid changes in total ozone, such as transient events in the lower stratosphere related to cyclonic disturbances in the troposphere. This results in a synthetic correlation between errors since the measurements tend to be either lower or higher than the model for some period of time (typically for a few days) due to an intrinsic 'memory' in the data. Another motivation for not worrying about AR-structure is that the model only accounts for roughly 50% of the variance of the raw data. This suggests that the model being used is incapable of describing the short term variations in the data and that it is the model itself that needs refinements, rather than the error structure. In the following models the method of generalized least squares was employed for estimating the model parameters and their statistical significance (for details, see the Appendix). Assuming independent errors does usually not affect the model parameters directly although the standard errors may be underestimated by not taking AR-structure into account.

Four types of the general model described by equation (1) are employed. Model of type I demonstrates the seasonal dependence of the solar- and QBO-effects on total ozone and can be expressed as:

$$O_3(t) = \alpha + \sum_{k=1}^{K} A_k \sin\left(\frac{2\pi k t}{365} + \phi_k\right) + \sum_{l=1}^{L} [\beta_l R_{t;t_0} + \gamma_l \mathrm{QBO}_t + \delta_l \mathrm{SOL}_t] I_{l;t} + e_t \tag{4}$$

where α is the overall long-term mean level and K is the number of harmonics used to model the annual variation, A_k is the seasonal amplitude and ϕ_k the phase of harmonic k. The parameters β_l give the magnitudes of the linear trends while γ_l and δ_l are the magnitudes of the ozone-QBO and ozone-solar relations, respectively. The function $I_{l;t} = 1$ if t falls within season number l and is 0 otherwise. $R_{t;t_0}$ is

given by

$$R_{t;t_0} = \begin{cases} 0 & \text{if } t < t_0 \\ t - t_0 & \text{otherwise} \end{cases} \tag{5}$$

so that no trends are assumed to be present before time t_0 (this is usually taken to be the time of the first observation within the period considered). The linear trends (β_l), QBO- (γ_l) and solar-parameters (δ_l) are thus fitted for each of the L seasons of the year.

In the next variant of the generalized model (type II) we perform a more detailed analysis of the seasonal behavior of linear trends by fitting different trend parameters for each month of the year:

$$O_3(t) = \alpha + \sum_{k=1}^{K} A_k \sin\left(\frac{2\pi kt}{365} + \phi_k\right) + \sum_{l=1}^{12} [\beta_l R_{t;t_0}] I_{l;t} + \gamma \mathrm{QBO}_t + \delta \mathrm{SOL}_t + e_t \tag{6}$$

where $I_{l;t}$ is now 1 if $t \in$ month l but 0 otherwise. This procedure yields more detailed variations of the trend parameters with the time of the year but the errors are larger. In the two models described above, no attempt is made to account for the shifts resulting from the intercomparisons made in 1977 and 1990. Therefore, care must be taken in selecting periods of the data for analysis. Data from different calibration periods can not be included in the same analysis.

The third model is constructed to reproduce the whole time series from 1957 to 1991 allowing for shifts in the mean on appropriate dates. Included are linear trends for each of the two first calibration periods. Since the last period is relatively short (one year), no attempt is made to model the linear trend there. This type of the model does not include seasonally dependent trends. Type III of the model can be expressed as follows:

$$\begin{aligned} O_3(t) \;=\; & \alpha \Big[1 + d_1 \left(\frac{t - T_0}{T_1 - T_0}\right) \theta(t;T_0)\theta(T_1;t) + s_1 \theta(t;T_1)\theta(T_2,t) \\ & + d_2 \left(\frac{t - T_1}{T_2 - T_1}\right) \theta(t;T_1)\theta(T_2;t) + s_2 \theta(t,T_2) \Big] \\ & + \sum_{k=1}^{K} A_k \sin\left(\frac{2\pi kt}{365} + \phi_k\right) + \gamma \mathrm{QBO}_t + \delta \mathrm{SOL}_t + e_t \end{aligned} \tag{7}$$

where $\theta(t;T)$ is the Heaviside function, i.e.:

$$\theta(t;T) = \begin{cases} 0 & \text{if } t < T \\ 1 & \text{otherwise} \end{cases} \tag{8}$$

In equation (7), T_0, T_1 and T_2 are the dates on which the three different intercomparisons where made in 1957, 1977 and 1990. The estimated drift between 1957 and 1977 is denoted by d_1 and s_1 is the estimated shift due to the recalibration in 1977. Similarly, d_2 and s_2 are the corresponding parameters for the latter period.

For reference, we also include the model of the International Ozone Trends Panel (IOTP) [NASA/WMO Ozone Trends Panel, 1988]. The IOTP model (type IV, with normally distributed and independent errors) is:

$$O_3(t) = \sum_{l=1}^{12}[\alpha_l + \beta_l R_{t;t_0}]I_{l;t} + \gamma \mathrm{QBO}_t + \delta \mathrm{SOL}_t + e_t \qquad (9)$$

where the annual variation is now modeled with different means within each month. Except for this, the model is similar to type II of our model. The data used for estimation of the parameters of this model are the monthly mean values of the original full data set. Each month is then weighted by its standard deviation, or the standard deviation for that month as estimated from the whole period (these two methods of weighing the data give very similar results).

Our trend analysis models can only be considered as diagnostic tools for evaluating possible long term changes in ozone. The influential factors determining the course of total ozone variations are specified at the outset and based on known or plausible physical mechanisms. With such prespecified variations, the model can accurately describe long term trends in the ozone data. When the models have been fitted to the data, the residual noise variance is generally about 40-50% of the total variance of the data. (or about 25% if monthly mean values are calculated). Figures 5a and 5b show how the trend model (type I) fits to the ozone data and the remaining residuals for the periods 1957–1977 and 1977–1990, respectively. The ratio of the variances of the residual and the data (σ_r^2/σ_d^2) is about 0.50 for the earlier period and 0.42 for the latter.

4 Results

4.1 The annual course of total ozone and temperatures

In Figure 6a we show the annual course of total ozone averaged over the two time periods 1957–1977 and 1977–1990. Figure 6b shows the temperature at the 30 and 100mb pressure levels averaged over the entire observing period. The annual ozone increase starts around the winter solstice, reaches a maximum near the spring equinox and gradually decreases for the rest of the year. This behavior reflects the well documented annual course of extratropical total ozone [see, e.g. London, 1980] and is a consequence of the dominant role of the mean meridional circulation in distributing ozone latitudinally (i.e. downward and poleward net transportation during the winter). This is consistent with relatively short dynamical time constants as compared with the chemical lifetimes of odd oxygen (O_3 + O^3P + O^1D) in the lower staratosphere [see, e.g. Brasseur and Solomon, 1986]. (The redistribution of ozone from regions of largest production was originally suggested by Dobson [1930]). The annual temperature change in the lower stratosphere is similarly a direct consequence of transport. Enthalpy (sensible heat) is supplied to the cold

	J	F	M	A	M	J	J	A	S	O	N	D
'57–'67	18.6	16.1	21.2	21.7	25.9	23.2	24.1	23.8	22.6	20.5	18.2	17.4
'68–'77	13.2	12.2	14.0	15.9	16.9	15.7	16.1	13.3	15.3	14.7	15.1	11.9
'77–'90	4.5	21.6	27.0	27.5	27.7	25.8	28.4	27.3	26.8	24.1	9.8	3.8

Table 1: Mean number of observations per month (periods of no operation excluded).

polar regions by the general circulation to balance the net radiative cooling during the winter. The process reverses during the summer season. Figures 6a and 6b clearly show increased variability in both total ozone and lower stratospheric temperatures due to increased wave activity (migrating weather systems) during the winter season. The apparently larger variability of total ozone for the latter period (1977 to 1990), however, reflects relatively fewer observations performed during the mid-winter for that period, as can be seen from Table 1, which shows the average number of observations made during each month of the year for three different time periods. Figure 6a also shows how the long term average of total ozone is affected by sudden stratospheric warmings. The general increase of total ozone during the spring is interrupted during the months of February and March. The stratospheric warmings are also evident in the long term temperature averages at the 30mb pressure level (ca. 24 km) while temperatures at the lower level 100mb temperatures (ca. 16 km) appear to be less affected. This is related to an observed decrease in the amplitudes of a typical warming composed of zonal harmonic wavenumbers 1 and 2 with decreasing height in the lower stratosphere [see e.g. van Loon *et al.*, 1973]. From Figure 6a it appears that sudden warmings occur about two weeks later in the spring during the latter period.

In Figure 7 we have applied a 10 day FWHM triangular filter to the daily averages of both the total ozone and temperatures at the 30mb pressure level over the entire observation period (i.e. 1957–1990). Sudden warmings in the stratosphere clearly have significant effects on the long term annual cycle of both total ozone and the 30mb temperatures, particularly during the periods November-December and February-March. Final stratospheric warmings also appear in the long term mean of total ozone in March and April, just preceeding the shift in circulation to the characteristic summer wind patterns with the preferred easterly zonal wind direction [e. g. Schoeberl and Hartmann, 1991].

4.2 Linear trends

In Figure 8 we show the whole data record of the monthly averages of total ozone at Reykjavik from July 1957 to August 1991. The record is nearly continuous in time and the missing data in 1960 leads to the largest gap in the record. The temporal behavior and the range of the data closely resembles the monthly means

of total ozone for the latitude belt $53° - 64°$ N. as published by Bojkov *et al.* [1990]. Figure 9 shows the deviations of the monthly means from the long term mean of total ozone. The upward shift in the data after the calibration in 1977 is apparent. To see how this can affect the relative long term annual total ozone behaviour we show in Figure 10 the long-term daily averages for the two seperate periods, smoothed with a 60 day FWHM triangular filter. The solid line denotes the earlier period and the upward shift for the latter is again evident. Up to 8% difference between the two periods appears in November. The two curves almost coincide during January and February, indicating a real decline (possibly 5%) in the average total ozone of the latter period as compared to the earlier. This could, however, be coincidental because of the increased natural variability of total ozone during the winter and relatively large errors in the few C and CD (ZB, ZC) observations. Figure 11 represents the deviations of the monthly means from the long term monthly means of the two separate calibaration periods. The overall trend is significantly more stable now and resembles the corresponding 100mb temperatures, shown in Figure 12, more closely. The temperature data do not indicate any sudden shifts occurring immediately after 1977. This strongly supports the conclusion that the data have to be separated into two distinctive calibration periods when studying the long term behavior of the total ozone data from Reykjavik. The rather large dip in the total ozone (roughly 10%) during the winter 1982-1983 may be associated with the eruption of El Chichon in 1982. This can also be seen from total ozone records at other Dobson stations at lower latitudes [see, e.g. Bojkov *et al.*, 1990]. The relatively low ozone values appearing in the early sixties could be attributed to nuclear weapons testing conducted in the atmosphere in the late fifties and early sixties as initially suggested by Chang *et al.* [1979]. The extremely low values during the last months of 1972 and the winter 1989/90 are possibly associated with large solar proton events (SPEs) as discussed in section 4.2. Other anomalies appearing in the deseasonalized monthly means of total ozone are mainly due to QBO effects, possibly El Niño events and erroneous winter values.

Physical mechanisms that mainly determine the ozone budget, such as prevalent circulation patterns and solar zenith angles, depend strongly on the season. When calculating linear trends, it is therefore desirable to consider each season or month separately. In the following, we present the seasonal or annual results since the calculated standard errors of the model parameters generally yield nonsignificant results on a monthly bases. In Figure 13 we present linear trends for three different seasons (winter: December-March; summer: May-August; fall: September-November, which is the same selection of seasons as in the WMO report, 1990), along with estimated standard errors ($\pm 2\sigma$) for types I–IV of the model. The linear trends and related errors are calculated from the residuals of the model calculations after the removal of the solar and QBO influences from the data. The agreement between types I, II and IV is excellent during the summer season for both time periods. During the winter and fall, the differences are higher but within the estimated errors of the models. The large error bars during the winter season reflect the difficult conditions

for measuring total ozone at low solar zenith angles with only a few measurements existing during this part of the year when variability of ozone is the highest (see Table 1).

In Tables 2 and 3 we summarize the model results of linear trends and corresponding standard errors for both periods. From the comparisons of the estimated linear trends of different variants of the general model (equation (1)) it is concluded that the differences in the results can be as large as two standard deviations of the estimated errors of the models (i.e. type I and II during the winter). This is related to the different estimates of the solar- and QBO signals in the two models. In the type I model the parameters corresponding to these influences are modeled as seasonally dependent, whereas a single annual average value is used in type II. The solar signal influences are largest during the winter (see section 4.4). Therefore, part of the estimated winter trend using model of type II may be due to solar effects which still remain in the residuals. This needs to be emphasized in all linear trend model studies of total ozone. Values of the linear trend parameters of type IV model (IOTP model) fall within the estimated errors of both type I and II models during the summer for both periods. During the winter and fall, however, linear trends of the type IV model are significantly different from the results of the other two seasonal models. This can be attributed to the effects of using the monthly averages instead of daily values when the data variability is large. The relatively large errors of type IV of the model are also due to the use of the monthly means of the original data set to represent the annual variation instead of the full data set. The Type III model, which fits the entire data set and allows for the shift in 1977, yields linear trends that represent well the annual average of the linear trends of the other models, thus strengthening the confidence in the results of the seasonally dependent linear trends. The estimated shifts, s_1 and s_2, are 4.5% and 3.2% for 1977 and 1990 respectively.

No definite linear trends are detected (at the 2σ level) except during the summer season and for the winter over the earlier period for both types I and II. Total ozone decreases by about $0.47 \pm 0.14\%$/year during the summer for the period 1977–1990 (Table 3) but increases marginally by about $0.08 \pm 0.13\%$/year for the 1957–1977 period (Table 2). The linear trend of the annual budget of total ozone is negative for both time periods (as estimated with model of type III), but the rate after 1977 is three times the rate in the period 1957 to 1977. The increasing annual rate of decline of total ozone during the last decade is in agreement with other trend studies [WMO, 1990] and could possibly be linked with human activities [Solomon, 1990].

The present results show that the summer decline during the latter period is largely responsible for the annual decline in ozone. No existing theory can account for such a large change in the total ozone amount during the summer season. A possible explanation of this phenomenon can be the redistribution of ozone poor air during the late spring (when the winds become more zonal) from regions at other longitudes that have been subjected to a more effective ozone-damaging chemical processing during the winter than occurring above Iceland. This suggestion is sup-

Linear trends [%/year]	type I	type II	type III	type IV
winter	-0.32±0.15	-0.42±0.11	-0.11±0.07	-0.23±0.40
summer	+0.083±0.13	+0.11±0.10		+0.11±0.18
fall	-0.068±0.14	-0.054±0.10		+0.11±0.24
Annual mean [DU]	331±3	331±3	328±2	336±4
QBO [DU/10m/s]				
winter	-1.9±1.9	-2.0±1.0	-2.3±0.7	-2.8±2.1
summer	-2.0±1.7			
fall	-0.33±1.9			
SOL [DU/100flux]				
winter	13.0±5.0	7.3±2.6	7.8±1.8	7.7±5.3
summer	6.4±4.3			
fall	2.9±4.4			

Table 2: Model parameters for the period 1957–1977. All uncertainties represent two standard errors (winter: DJFM; summer: MJJA; fall: SON).

ported by the zonally averaged ozone decline during the earlier part of the year (0.6%/year) as derived from the TOMS data (see section 4.3). The frequent North Atlantic lows during winter may be a significant contributing factor in supplying ozone as well as sensible heat into the region and thus averting significant ozone loss. At the pressure of 30mb and typical stratospheric mixing ratios of water vapor and HNO_3 species, laboratory studies suggest [Hanson and Mauersberger, 1988] that temperatures below -80°C are required to form the crystalline phase of the nitric acid trihydrate, particles that comprise most of the PSCs [Fahey, 1989]. Still lower tempearatures are required to form ice particles (a frost point temperature of -87°C for the same conditions). Inspection of the temperature record at the 30mb pressure level above Keflavik for the entire period 1957 to 1991 shows that only on rare occasions (one, or at the most a few days at a time) do temperatures drop below -80°C. This is in contrast with balloon measurements made at Kiruna, Sweden (68°N, 21°E) during the winter 1989 to 1990 [Hofmann and Deshler, 1991]. Temperatures between the 70mb (17km) and 20mb (27km) pressure levels dropped well below -80°C and lasted for many days in January and February. The formation of PSCs may, therefore, be a rare event above Iceland as compared to other regions at similar latitudes and prevent heterogeneous chemical reactions to proceed at a rate fast enough to cause significant release of Cl radicals and subsequent ozone destruction. This suggests that non-local effects on ozone changes during the winter have to be taken into account when assessing the observed summer decline of total ozone at Reykjavik.

Out of a total of 19 Dobson stations suitable for trend analysis and located northward of 40°N only Sapporo, Japan (43°N) shows a similar non-significant win-

Linear trends [%/year]	type I	type II	type III	type IV
winter	+0.17±0.23	-0.039±0.19		+0.54±0.85
summer	-0.47±0.14	-0.46±0.12	-0.30±0.11	-0.51±0.31
fall	-0.097±0.18	+0.021±0.15		+0.084±0.46
Annual mean [DU]	340±3	345±3	343±6	352±6
QBO [DU/10m/s]				
winter	-0.9±2.3			
summer	-1.6±1.3	-2.2±0.9	-2.3±0.7	-2.6±2.2
fall	-0.33±1.8			
SOL [DU/100fu]				
winter	28.8±5.7			
summer	9.3±3.7	9.9±2.4	7.8±1.8	9.0±6.0
fall	0.94±4.1			

Table 3: Model parameters. Same as Table 2 for the period 1977–1990.

ter decline in ozone. Results from the two other Japanese Dobson sites, Tatento (36°N) and Kagoshima (31°N), show comparable wintertime tendencies, as well as the regional average derived from the Far Eastern M-83 filter ozonomerers [WMO, 1990]. Since no instrumental problems have been identified, it is concluded that the most plausible explanation is that the sampling is made in a different meteorological regime than over most other northern continental regions. Lower stratospheric climatological charts show the jet stream passing over the area in almost a meridional direction, thus leading cylcones with associated northward transport of ozone and sensible heat into the region. Similarly, the North Atlantic region is favoured for the same insertion by synoptic events associated with the arctic jet stream. The two far apart regions may therefore be refrained from the effective wintertime ozone-damaging chemical processes apparently taking place at other regions at similar latitudes. More quantitative studies are needed to signify the role of synoptic small scale dynamical events in determining total ozone trends.

The apparently larger decline of ozone during the winter for the earlier period (roughly 0.36%/year) as compared to the latter, which shows no significant change, can be attributed to large existing longitudinal gradients in total ozone that are shifting with time. The delayed occurrences of sudden stratospheric warmings during the early spring for the latter period (see Figure 6a) suggest that the prevalent long term climatic conditions above Iceland have been changing over the last three decades. This needs to be investigated further.

Figure 14 shows the zonally averaged linear trends from previous studies at this latitude by Bojkov *et al.* [1990] and Stolarski *et al.* [1991]. The former study is based on the Dobson network for the latitude belt 53°N–64°N over the period 1958–1986 while the latter uses the TOMS satellite data. The two differ significantly and are

also different from the results of this study. The TOMS data show that the zonally averaged total ozone during the winter has been rapidly declining ($7.8 \pm 3.9\%$) over the last 13 years which is in contrast with the present results for Reykjavik ($2.2 \pm 3.0\%$ increase for type I model). The present model results for the fall season show no significant linear trends. This agrees with the results of Bojkov *et al.* [1990], but appears to be (marginally) different from the behaviour of the TOMS data which shows a significant decline for this season. This indicates, as mentioned earlier, that the zonal average does not necessarily represent local changes and long term linear trends of total ozone during the winter and fall seasons may be very different from one region of the atmosphere to another at high latitudes in the northern hemisphere. The zonally averaged summer decline derived from the TOMS data is in good agreement with the present results.

Figure 15 shows the total ozone deviations (in DU) from a long term mean for all seasons and both time periods after the data have been adjusted for the seasonal, solar and QBO influences. The general negative trend during the summer for the latter period is apparent from the residual with the largest downward trend occurring in 1990. The deviations seem to be relatively larger during the earlier period, suggesting higher quality data after 1977. The observed large decline of total ozone during the winters 1963/64 and 1964/65 is possibly related to atmospheric nuclear tests during the late 1950's and early 1960's. This is concurrent with modeling studies [e.g. Wuebbles, 1983] and the primary testing period in 1961 and 1962. The large dips in ozone during the winter 1982/83 may be associated with the El Chichon eruption, as discussed earlier.

The lowest residual values in Figure 15 appear in the fall and winter of 1972 and during the winter of 1989/90. Both anomalous values occur just after the two largest SPEs on record over the last three decades (August 1972 and October 1989). Large depletions of ozone are predicted to follow a major SPE in the upper stratosphere and mesosphere and have been interpreted as a direct response to the HO_x related chemistry with relatively short response time scales (one day or less). Theoretical predictions seem to agree fairly well with observed ozone depletion [Solomon *et al.*, 1983]. Significant ozone depletion in the stratosphere was also observed by the Nimbus 4 satellite immediately after the August 4, 1972 SPE and is believed to be related to the longer lived NO_x chemistry in the lower stratosphere. The large decline of total ozone in the present study (roughly 70DU or 25%) following the two major SPEs has not been clearly identified before by the Dobson network. The TOMS data indicate no significant sudden changes in the total ozone following the SPE in 1989 [see Figure 17b]. The timing of the two events as measured by the Dobson at Reykjavik just after the SPEs is hardly coincidental but the lack of agreement with the TOMS data needs to be explained. The present results should be a motivation for further investigation of the interesting relation of SPEs to ozone changes.

4.3 Comparison with TOMS

Comparing the data and modeling results with the TOMS data over the last 13 years provides an opportunity to evaluate the significance of the present study. The TOMS data used are from measurements made while the satellite is directly overhead the ground-based Dobson station at Reykjavik. Figure 17a shows such a comparison made for the monthly means when at least 10 days with both Dobson and TOMS observations are available and the differences in the solar zenith angles of the satellite and the ground-based station agree to within 5 degrees. The results show that the precision of the ground-based data relative to the TOMS data is very high, and is actually among the highest of all Dobson stations of the world [e.g. Bojkov *et al.*, 1988], which confirms the high quality of the Reykjavik data. The shift appearing in the last part of the comparison series (1990–1991) is due to the recalibration of the Dobson instrument in July-August 1990. This part of the data is excluded in what follows. The calculated difference of the two data sets relative to a common baseline is 3.6% (2σ of the absolute differences). This is about the same as the accuracy of the comparison which is about 3.4% if a value of 1.5% (2σ) is used for the estimated errors of the TOMS data over a 13 year period, as suggested by McPeters and Komhyr [1991], and 3.0% for a good ADDS measurement. The relative drift calculated by fitting a line to the data in Figure 17a, excluding the data after the calibration in 1990, is about -0.75% over the entire time period and thus insignificant. This suggests that the influence of possible increase of tropospheric ozone below about 5km (the height at which the satellite becomes insensitive to ozone changes [Stolarski *et al.*, 1991]) is not influencing the present results of linear trends in the annual total ozone amount. The magnitude of the apparently constant shift in absolute values is in accordance with the study made by McPeters and Komhyr [1991] based on an ensamble of 39 Dobson stations worldwide. The results after the recent calibration in July-August 1990, however, look somewhat suspicious, showing very high ozone values at the end of the record. A detailed comparison of relative shifts in absolute total ozone values is beyond the scope of the present study. When including all the Dobson values in the comparison, the agreement with the TOMS data diminishes (Figure 17b). This is due to the few and unreliable observations made during the winter and the sensitivity of derived total ozone amount on the μ value (the relative slant path of the solar beam through the center of gravity of the ozone layer). Figures 18a-d show comparisons with the TOMS data for different wavelength pairs, AD, CD, CC′ and C. The larger dispersion of the differences at higher solar zenith angles is particularly evident for measurements made at the C and CD wavelength pairs.

Because of the excellent agreement of the total ozone at Reykjavik and the TOMS data, this station provides confidence in the satellite data and could serve as a ground-based reference data set for the TOMS results at high northern latitudes and thus help determine what techniques for determining and removing drifts in the calibration of instruments are realistic. During the winter (December and

Linear trends [%/year]	type I	type II	type IV
winter	+0.16±0.16	-0.15±0.14	-0.15±0.56
summer	-0.43±0.17	-0.37±0.15	-0.49±0.31
fall	-0.43±0.17	-0.37±0.15	-0.22±0.42
Annual mean [DU]	354±3	353±3	361±6
QBO [DU/10m/s]			
winter	-8.8±1.8	-4.7±1.0	-2.8±2.2
summer	-1.8±1.7		
fall	-3.9±1.8		
SOL [DU/100fu]			
winter	17.6±3.8	8.0±2.3	3.9±5.5
summer	5.7±4.5		
fall	-1.8±3.9		

Table 4: Model parameters deduced from the TOMS data (1978–1991).

January), however, a careful comparison of the two data sets is not warranted. At large solar zenith angles (greater than 80°) both the TOMS and the Dobson data become unreliable. The larger errors in the TOMS data are probably caused by a higher dependence on the background standard profile of ozone used in the retrieval algorithm when the effective reflecting surface will be elevated at higher solar zenith angles.

The linear trends of the TOMS data for different seasons of the year are shown in Figure 19 and Table 4, where type I, II and IV models have been applied to the data. Constant weights were used when modeling this data. When compared to the results for the Dobson measurements in Reykjavik (see Figure 13b) the linear trends during the summer appear to be almost identical and only marginally different during the winter. The TOMS data, however, show a significant decline during the fall and winter. The apparent differences in linear trends of the TOMS data and the data from Reykjavik during the fall are larger than would be expected from the observed (about 10%) annual increase in tropospheric ozone over the last decade [Bojkov, 1988]. The maximum expected increase in total ozone due to increased tropospheric ozone in the lowest 5km would be about 1% over a 10 year period in the northern hemisphere [Stolarski *et al.*, 1991]. Since polar stratospheric cloud occurrences are rare during the fall season at this latitude, the rapid zonally averaged decline is hard to account for. Changes in the prevalent long term dynamical conditions are the most plausible explanation. This phenomenon, including the relatively stable ozone layer above Reykjavik during the fall, needs to be studied in more detail.

When comparing the local and zonally averaged linear trends of the TOMS data (Figure 14 and 19) large differences appear in winter. This can be explained by large regional differences of total ozone changes in the stratosphere (see section 4.2).

4.4 Solar cycle and QBO influences

Based on the entire observing period (using the type III model) the established relationship of ozone with the 10.7cm solar flux is 7.8 ± 1.8 DU (Dobson units) per 100 units of $F_{10.7}$ or $3.5 \pm 0.8\%$ over a solar cycle (150 flux units). On the average, ozone changes by 2.3 ± 0.7 DU per 10m/s of the QBO windspeed. This amounts to about $2.1 \pm 0.6\%$ over one QBO. Both the QBO and solar signals are slightly stronger than reported by the WMO Ozone Trends Panel for the same latitude ($2.2 \pm 0.8\%$ and $1.8 \pm 0.31\%$ for the QBO and solar signal respectively).

Bojkov *et al.*, [1990] calculated about 2.6% change of ozone per 100 flux units from the published total ozone data as measured at Reykjavik for the period 1957 through 1986. This was found to be the strongest ozone-solar relation from a set of 28 Dobson stations located between 19°N and 64°N [see also WMO, 1990]. No apparent general relationship to latitude was found which is in contrast with the findings of the WMO Ozone Trend Panel and the work of Reinsel *et al.*, [1987] both of which indicate a considerably stronger solar signal in the data at higher latitudes. Further examination may be needed in determining the regional differences.

Calculating the ozone-solar cycle relation on a monthly bases leads to non-significant results because of the large estimated standard errors. However, there is an exceedingly strong dependence of the solar effect on the seasons as can be seen from Tables 2–4. During the winter the solar signal is about two to three times stronger than during the summer when it is comparable to the annual average. No influences are calculated for the fall season. Comparison of the two separate periods of the analysis shows that during 1977–1990 the solar cycle signal is about two times more influential than during the earlier period of 1957–1977. This can be ascribed to the relative average increase of solar activity during the latter period (see Figure 3). To examine further the high dependence of the solar signal on the season and possible QBO influences the data was averaged for each month and then divided into two separate sets according to the phase of the QBO over the whole period of observations. The shift in the data due to the unsettled calibration in 1977 was accounted for by shifting the data before 1977 upwards by $s_1 = 4.5\%$, this shift being deduced from the model of type III. The monthly mean data was then correlated with the mean sunspot number for each month. The strongest solar signal found is in February and in the westerly phase of the QBO when the correlation coefficient is $r = 0.73$ at the 99.9% significance level. Noticeable solar signal is also found in March for the same phase of the QBO ($r = 0.69$), but the signal is much weaker for all the other months. In the east phase of the QBO no correlation exists between ozone and the sunspot number in February ($r = 0.19$). In Figures 20a-b we show graphically how the 11.2 year solar cycle can influence total ozone behavior at this latitude in February. Total ozone can vary by as much as 25% during this month in the westerly phase of the QBO while no apparent dependence on the sunspot number is detected in the east phase.

No current theory can account for this seemingly large amplitude response of

total ozone in February to the solar cycle and only in the west phase of the QBO. Two dimensional model simulations by Brasseur *at al.* [1988] suggest that the responsive changes in ozone to observed relative solar cycle changes in the solar UV-irradiance are limited to about 1–2%. This is an order of magnitude smaller than indicated in Figure 20a. The largest percent changes, however, are also found in the early part of the year at high latitudes. Most of the solar influences appear to be associated with altitudes between 35 and 45km, well above the height of maximum ozone concentration. Other previous studies of short and long term effects of UV flux changes [e.g. Garcia and Solomon, 1984; Keating *et al.*, 1985; Hood, 1986] show similar results, and thus differing significantly from the findings of this study.

The apparently close relationship between total ozone and sunspot numbers during the early part of the year and only in the westerly phase of the equatorial QBO winds at the 50mb level has not been established before. The reason is partly due to the exceptionally long record of total ozone data available at this station and the relatively strong solar cycle signal found at the this high latitude observing station as compared to other Dobson stations. However, extratropical ozone and stratospheric temperatures have been known to exhibit strong relation to the QBO [e.g. Angell and Korshover, 1978; Oltmans and London, 1982; Hasebe, 1983]. Influences of solar activity on the 30mb polar temperatures in the west phase of the QBO have been reported by Labitzke [1987]. This is concurrent with the high ozone-temperature relation found in the west phase of the QBO in February of the present study ($r = 0.85$ at the 30mb pressure level for the monthly mean but lower for all other months). A corresponding 13.6°C temperature change over one solar cycle was calculated from the temperature data as measured at Keflavik at the same pressure level, the correlation coefficient being 0.65. Predicted temperature changes over one solar cycle only amount to a few tenths of a degree at this pressure level during the winter [Brasseur *et al.*, 1988]. The temperature correlation with ozone is somewhat lower in the east phase of the QBO ($r = 0.73$) but no relation to the sunspot numbers is found ($r = 0.15$).

The outstanding difference of total ozone behavior in the east and west phase of the equitorial QBO suggests that solar cycle influences at high latitudes can be strongly amplified under conditions determined by global dynamics. While no convincing physical mechanism has been proposed to explain the apparently significant temperature-solar relationship, Labitzke and van Loon [1988] have suggested that the planetary wave structure of the atmosphere is modified by the solar cycle influences on the phase of the QBO. As originally suggested by the work of Holton and Tan [1980], arctic temperatures and the strength of the polar vortex appear to be associated with the direction of the equitorial zonal winds at the 50mb pressure level. Labitzke [1987] suggests that the occurrances of major stratospheric warmings are dependent on the phase of the QBO such that no major warming occurs in the westerly phase of the QBO when the sunspot number is lower than 110. To investigate further the connection of stratospheric warmings and local changes in total ozone we have marked in Figure 20 the years of major warmings occurring in

February. While there appears to be a general agreement with the earlier work of Labitzke [1987] using the 30mb temperatures over the North Pole, the strong stratospheric warming in February 1987 when the sunspot number is low contradicts the earlier findings. This underscores the complexity of the problem and the difficulty in identifying a real physical connection between sunspots, the QBO and stratospheric warmings to upper air temperatures and total ozone. It is very likely that the strong ozone-sunspot relation revealed in Figure 20 is related to stratospheric warmings when the poleward flow of ozone rich air and sensible heat is effective. Sophisticated three dimensional and fully coupled general circulation models are problably needed to quantify the exact cause of this subtle phenomenon.

The variability and long term decline of antarctic ozone as related to the QBO was first suggested by Garcia and Solomon [1986]. Several studies have examined experimental data to verify the hypothesis [Lait *et al.*, 1989; Angell, 1990; Newman *et al.*, 1991). Close relationship of PSCs with the QBO in antarctic ozone and stratospheric temperatures have also been reported [Poole *et al.*, 1989]. The statistical significance of some of these studies are still marginal and there is a need for further modeling studies to substantiate this important effect, both to guide research campaigns and to predict future ozone changes.

5 Summary

The 34 year long data set of the near-continuous high quality total ozone Dobson measurements at Reykjavik truly represents an 'archaeological' record. The record extends the information on changes in total ozone, inferred from satellite data, some 20 years further back in time. In this paper we report on the results from analysis of this important Dobson station situated at the edge of the polar winter vortex. A careful scrutiny was applied to the station's record before trends in the data were determined. This included corrections due to the use of erroneous cloud transfer tables, identification of some badly performed measurements and typographical errors in the daily logbook and examination of the instrument's calibration. The reevaluation of the cloud transfer tables produced a new relationship of the CC′ with the AD direct sun wavelengths resulting in an overall change of 0.5-2.5% of total ozone values before 1977. Our trend analysis is based on two separate periods of the record (i.e. 1957 to 1977 and 1977 to 1990). This is due to problems related to the calibration of the instrument in 1977, producing a superficial shift in the published data not detected in the deseasonalized temperatures of the 100mb pressure level.

A statistical model was developed to accurately describe long term trends in the total ozone data. The phase and amplitude of the equatorial QBO and the solar cycle are known to be important in determining the total ozone behavior. These natural influences are included in the model by allowing a linear dependence upon the observed time series of the variations. The seasonal changes are well reproduced by a superposition of four harmonics. After having removed the natural variations,

linear trends and related standard errors are calculated for the residuals. Several different types of the model are applied to the data to see how the results are dependent on the exact form of the model and to compare our results to previous studies. When linear trends are considered, the different types of models agree well for summer and fall. During the winter however, when solar cycle influences are large, significant differences appear in the estimates of the linear parameters of models allowing for seasonally dependent solar influences and those including only a single annual average value of the solar parameter. The latter type will not ensure the adjustment for the strong solar signal during the early part of the year.

The most significant result found in the linear trends is a calculated decline of $0.47\pm0.14\%$ per year (at the 95% confidence limit or two standard errors) during the summer season from 1977 to 1990. The annual total ozone amount declines at the rate of $0.30\pm0.11\%$ per year over the same period which is about three times the rate of decline over the earlier twenty years of observations. This change is reflected by the large summer decline since no significant decline (at the 2σ level) is deduced for the winter and fall seasons during the latter period. When linear trend parameters of our models are compared with the zonally averaged trends at this latitude inferred from data of both the ground-based Dobson network and the Nimbus 7 (TOMS) satellite, large differences are found during the winter. No significant decline is detected at Reykjavik but seemingly a very large decline of the zonal average is observed by the TOMS (0.6%/year). Since the agreement is excellent during the summer it is concluded that the noteworthy summer decline of total ozone at Reykjavik is a consequence of a diffusive processes indicative of large ozone destruction occurring at other regions at high northern latitudes during the winter season. Observed differences in climatological conditions with longitude support this suggestion.

Comparison of the data at Reykjavik with the TOMS data for the period 1978 to 1991 generally show an excellent agreement (within the accuracy of the comparison) for solar zenith angles of less than 80° with no significant relative drift appearing in the long term differences. This suggests that the Dobson spectrophotometer situated at Reykjavik could be used as a reference for the TOMS measurements at high latitudes. During December and January the two data sets differ considerably due to unfavourable observing conditions for both measuring devices. Linear trends deduced from the models using both sets of data agree very well, the largest difference (marginally significant) appearing during the fall.

Solar cycle influences at this location are apparently stronger than observed in other regions in the northern hemisphere. The exceptionally long record of good quality data may be the reason for a successful detection of an unprecedent strong solar control of total ozone during the early part of the year and only in the westerly phase of the QBO. Up to 25% of the total ozone variability in February can be referred to solar cycle influences. Correspondence with previous work of Labitzke [1987], relating northern polar 30mb temperatures to sunspots, can be made on the bases of the strong total ozone-temperature correlation (at the same pressure level)

during this month. No successful physical hypothesis for this phenomenon has been proposed. Due to the complexity of the problem, three dimensional fully coupled radiative-dynamical and chemical atmospheric models may be needed to successfully reproduce this important effect.

The notable and possibly accelerating ozone decline in the nortern hemisphere due to the release of ozone-damaging chemicals by humans is expected to be most effective during the early part of the year. A thorough understanding of the natural variability, including solar cycle influences, during this season is essential for a quantitative estimate of ozone decline in the upper atmosphere.

The findings of the present study are considerably different from the reported results of the International Ozone Trend Panel analysis for the latitudinal belt of 53°N to 64°N, particulaly during summer.

6 Acknowledgements

We are grateful to Guy Brasseur for giving one of us (Ö. E. R.) the opportunity to use the facilities at NCAR. We thank Richard McPeters for providing the TOMS data for the geographical location of Reykjavik. The help of Borgthor H. Jónsson in making the temperature data at Keflavik available to us is acknowledged. This work was supported by the Icelandic Science Council, NATO, Icelandic Alloys Ltd., the Atmospheric Chemistry Division of NCAR and the Nordic Council of Ministers.

7 Figures

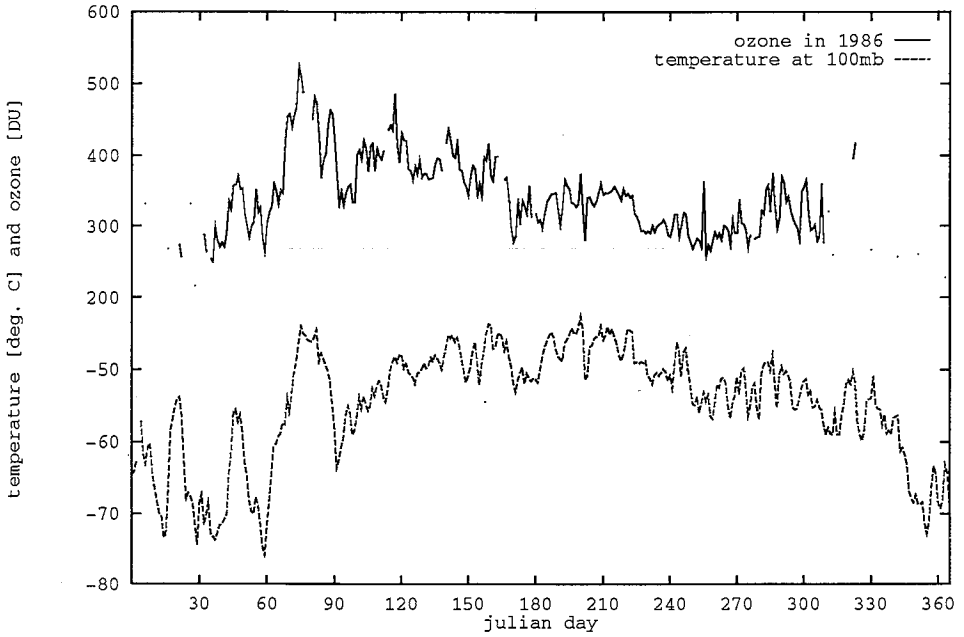

Figure 1: Daily measurements of ozone and 100mb temperature in 1986.

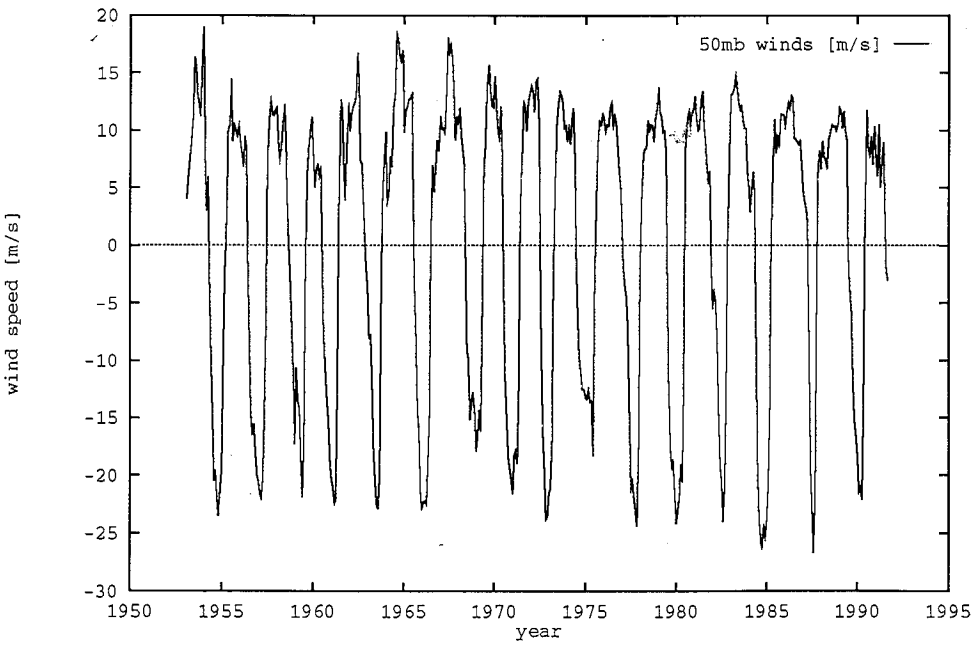

Figure 2: Monthly mean zonal wind speeds at the 50mb pressure level at Canton Island (2°46′S, 171°43′W), Maldives (0°41′S, 73°09′E) and Singapore (1°22′N, 103°55′E). Ticks mark the beginning of each year.

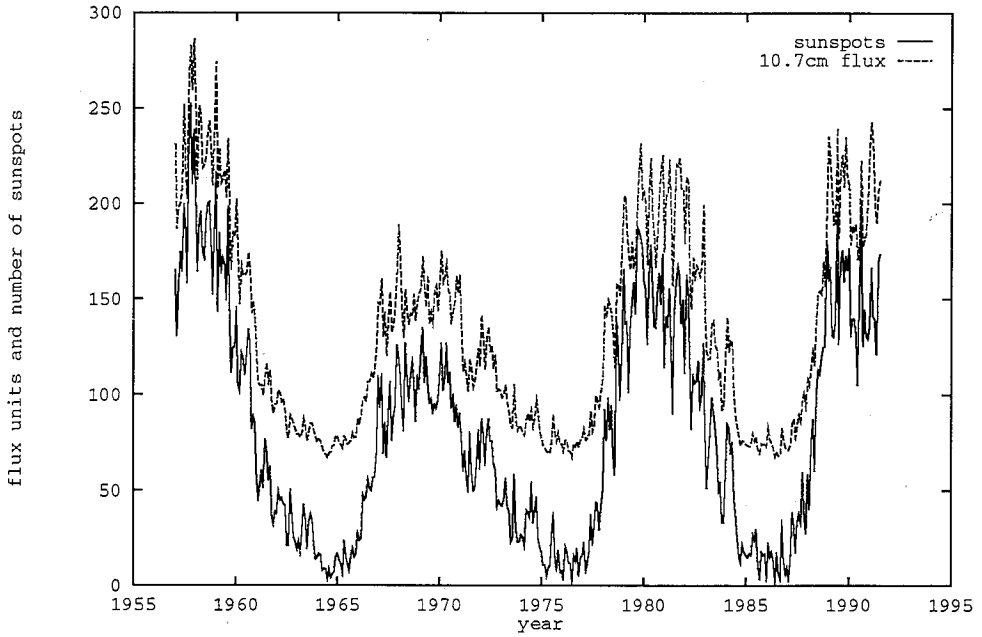

Figure 3: Monthly mean values of sunspots (solid line) and the 10.7cm solar flux (dashed line).

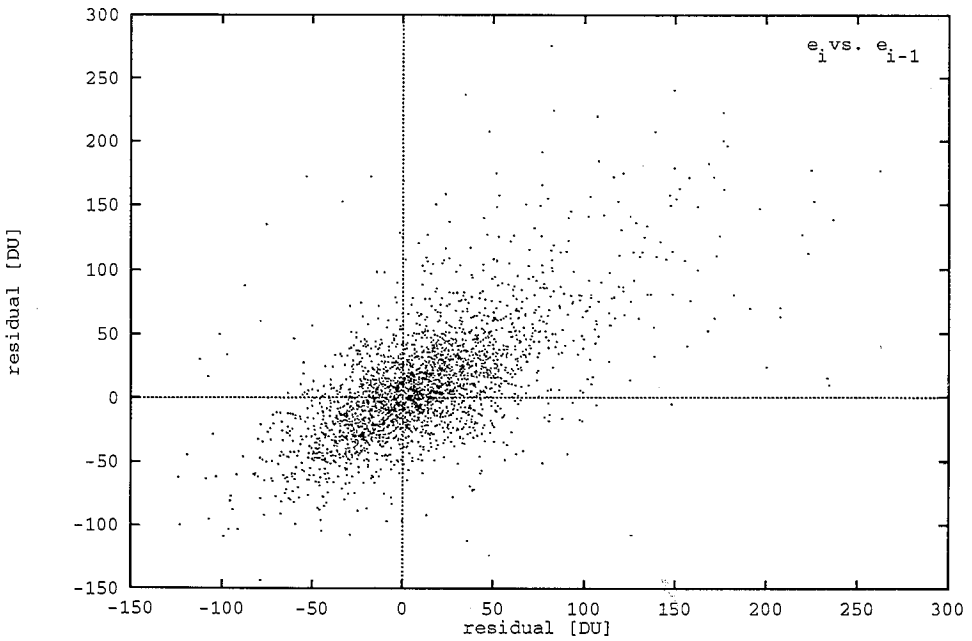

Figure 4: Residuals at time t as a function of residuals at time $t-1$.

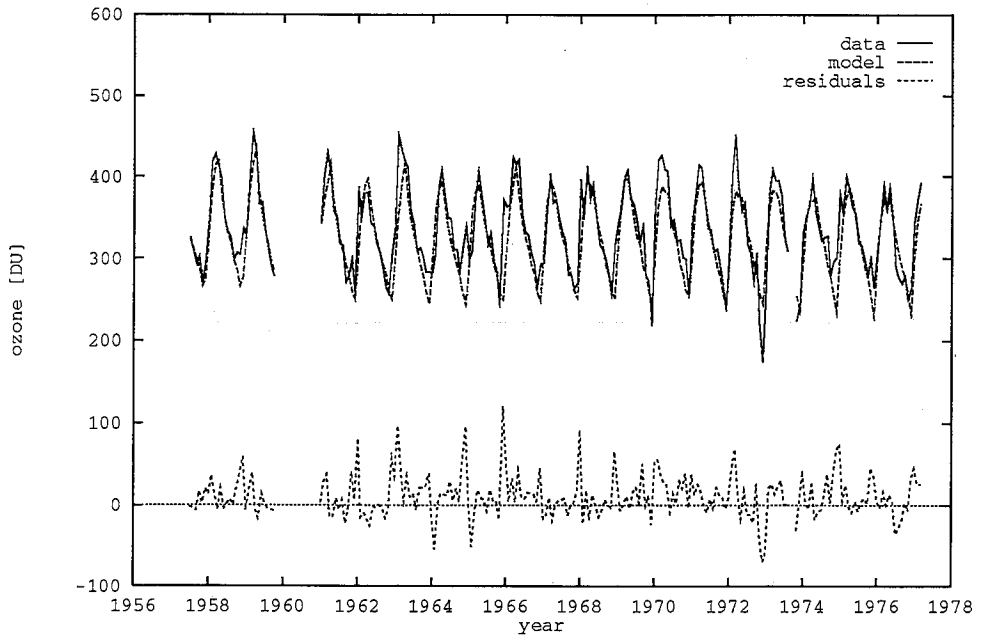

Figure 5a: Comparison for the period 1957–1977 between model, type I, (dashed line) and data (solid line) after monthly averages have been calculated. Also shown are the remaining residuals.

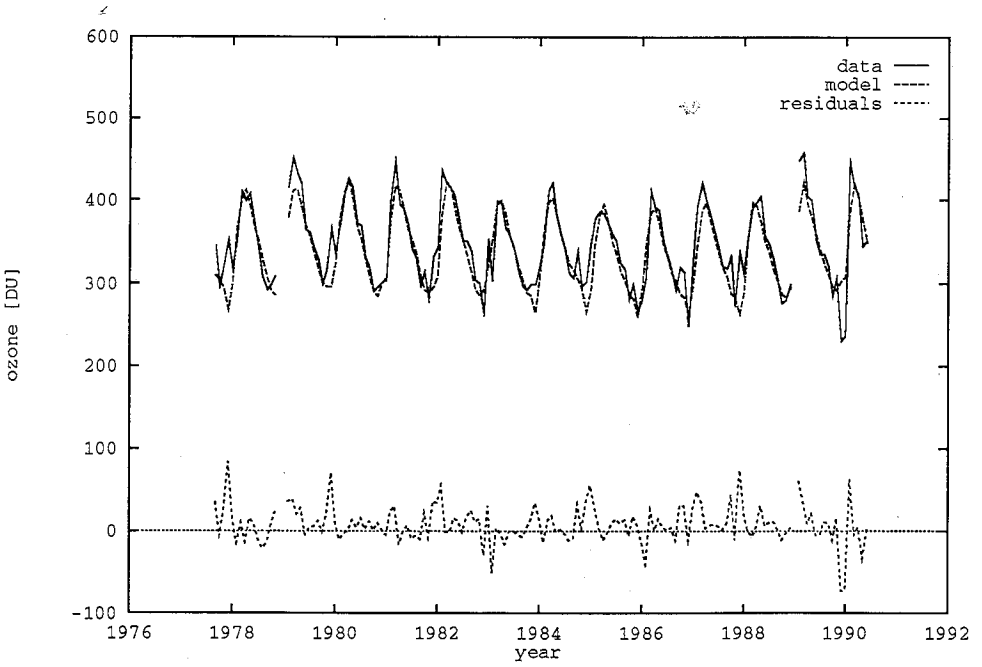

Figure 5b: Same as Figure 5a, except for the latter observing period (1977–1990).

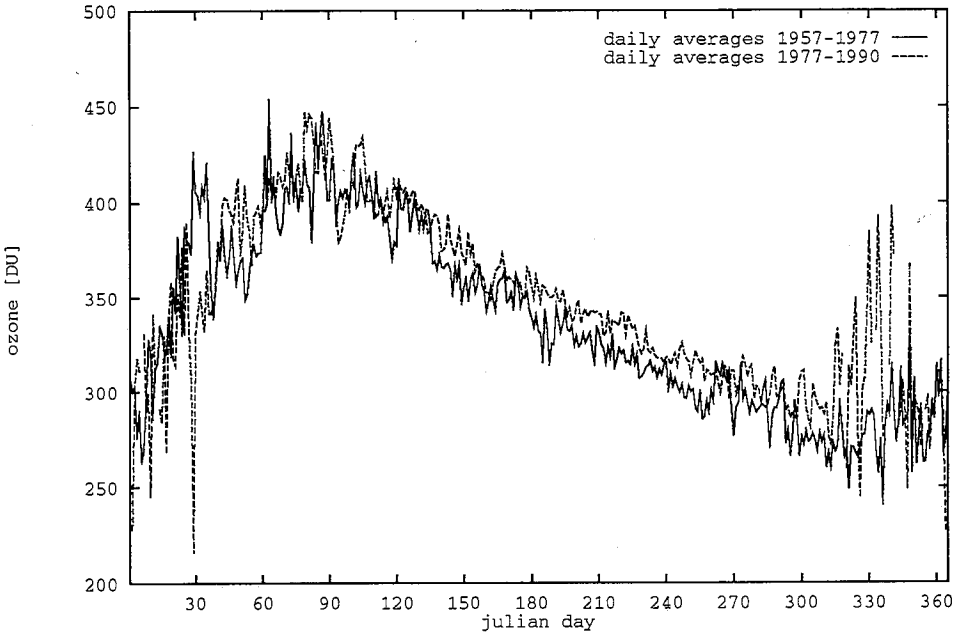

Figure 6a: Annual course of daily values of total ozone averaged over the two observing periods, 1957–1977 (solid line) and 1977-1990 (dashed line).

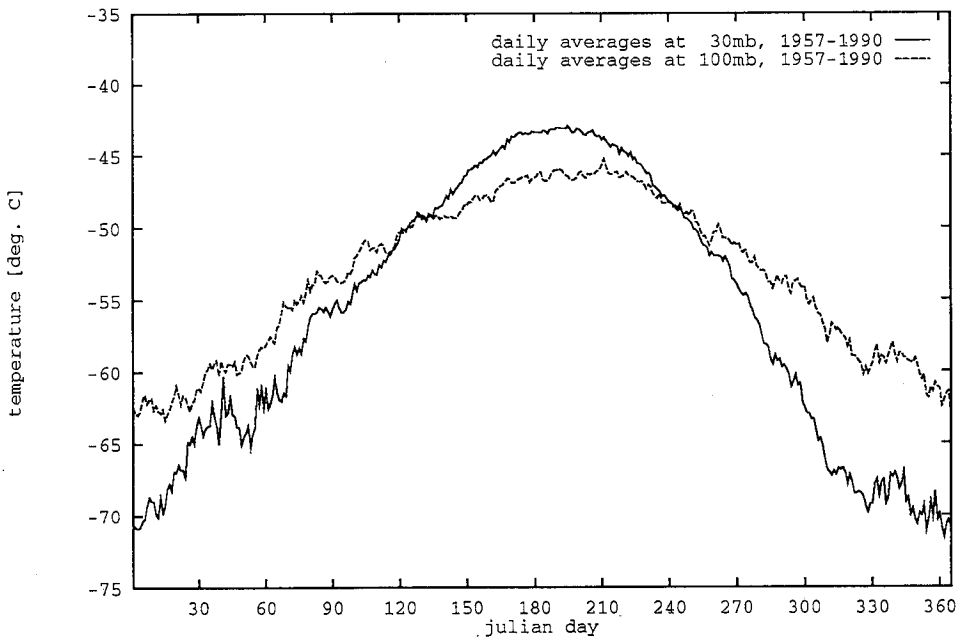

Figure 6b: Annual course of temperatures at the 30mb (solid line) and 100mb (dashed line) pressure levels averaged over the entire observing period.

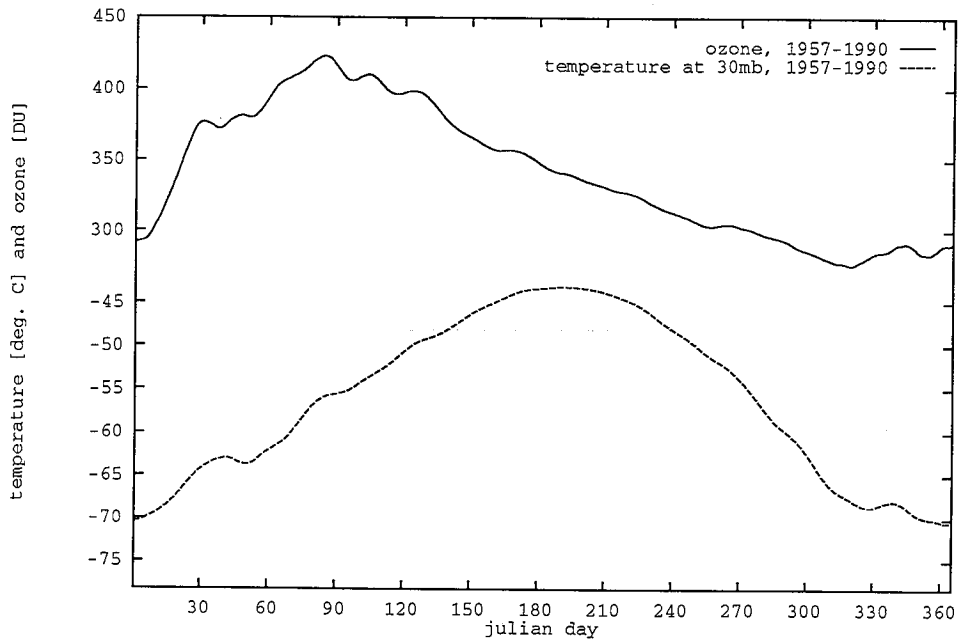

Figure 7: Mean annual course of total ozone and temperatures at 30mb for 1957–1990. The data has been smoothed with a 10 day FWHM triangular filter.

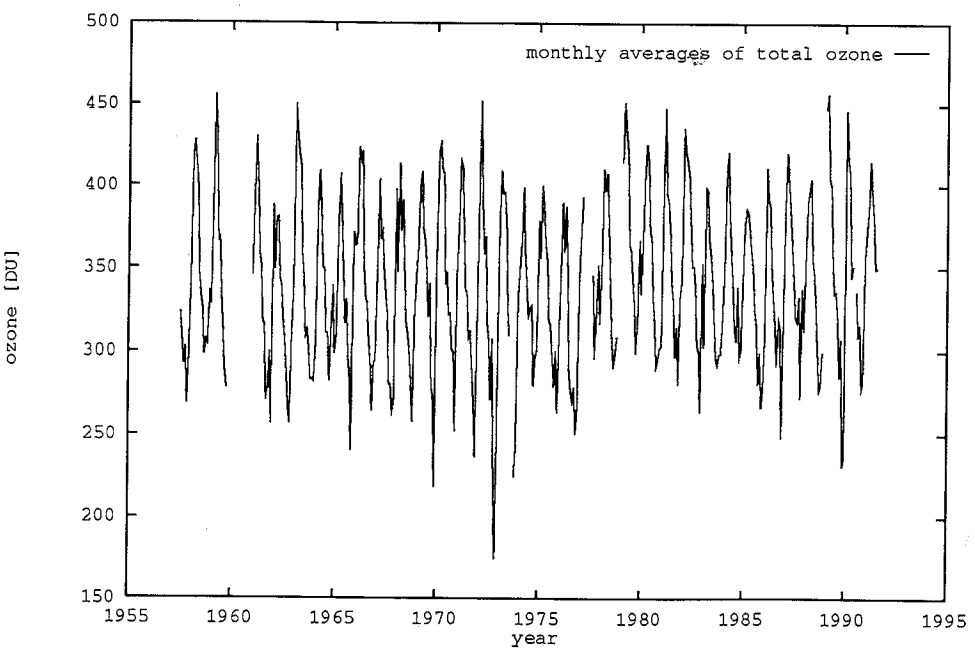

Figure 8: Data record of total ozone at Reykjavik (monthly averages).

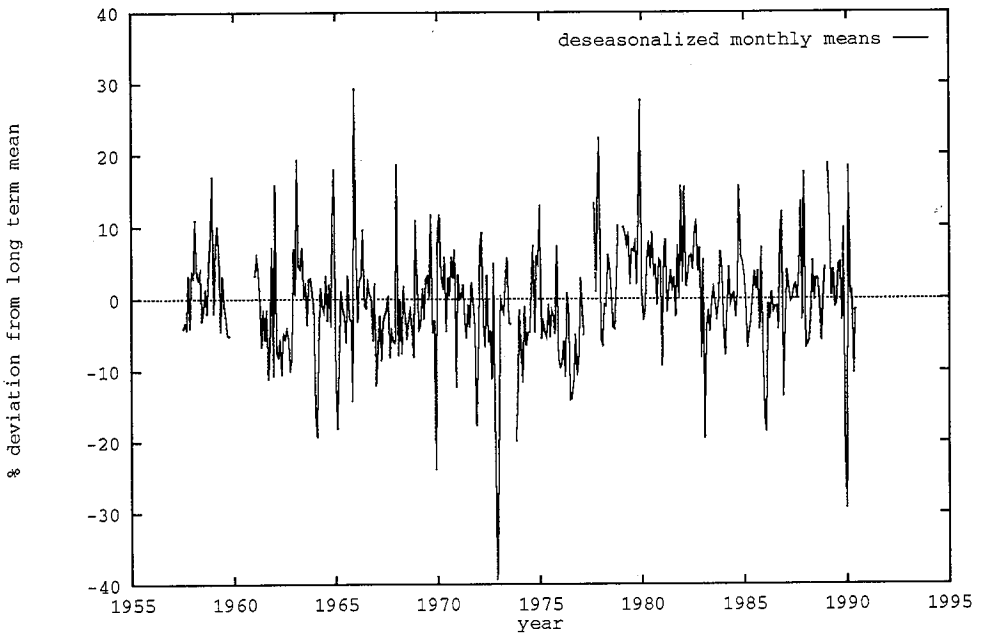

Figure 9: Deviations of the monthly means from the long term mean of total ozone. Note the upward shift in the data after the calibration in 1977.

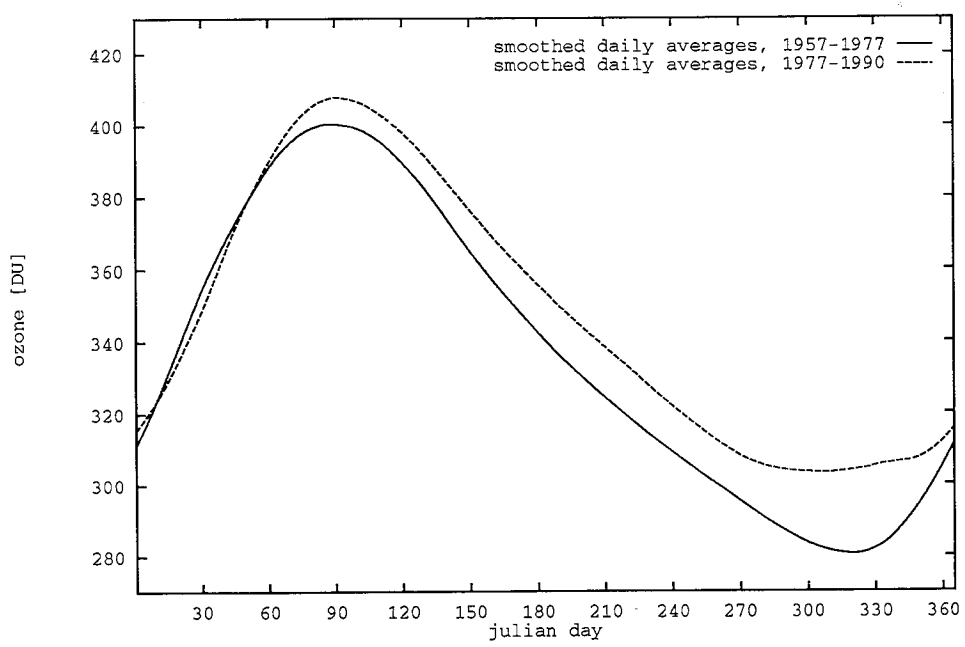

Figure 10: Long term daily averages of total ozone for the two periods (1957–1977, solid line and 1977–1990, dashed line), smoothed with a 60 day FWHM triangular filter.

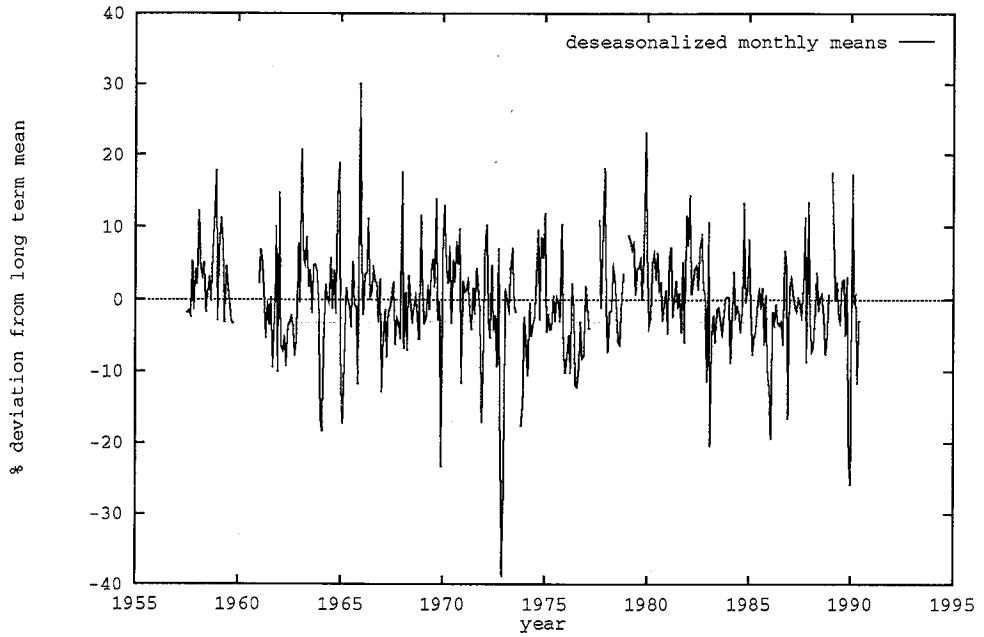

Figure 11: Deviations of the monthly means of total ozone from the long term monthly means of the two separate calibration periods.

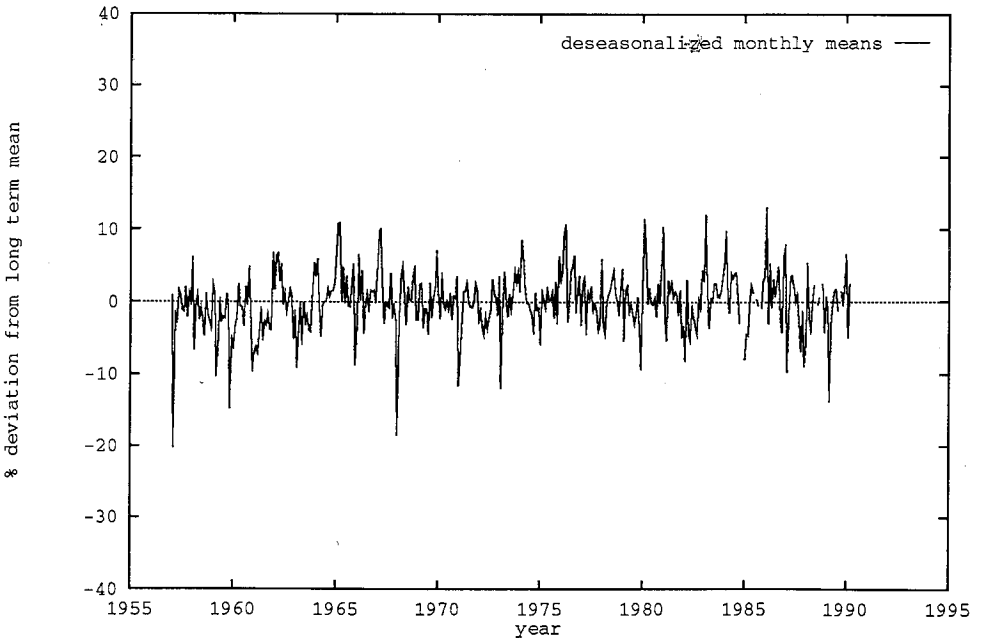

Figure 12: Same as Figure 9, except for temperatures at 100mb.

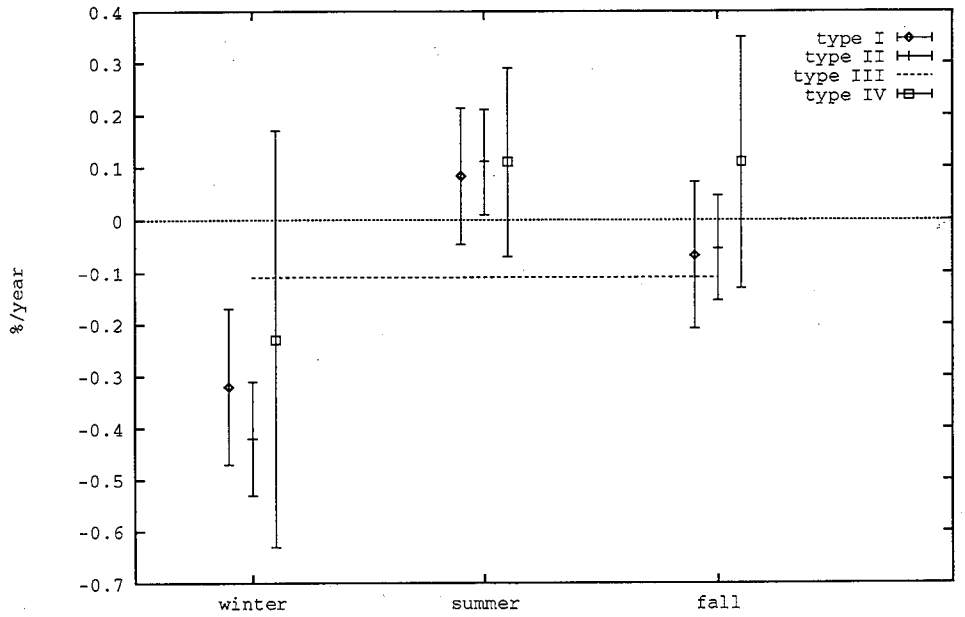

Figure 13a: Linear trends during 1957–1977, for the three different seasons along with estimated standard errors ($\pm 2\sigma$) for types I-IV of the model. Winter denotes December through March, summer is May-August and fall is September-November.

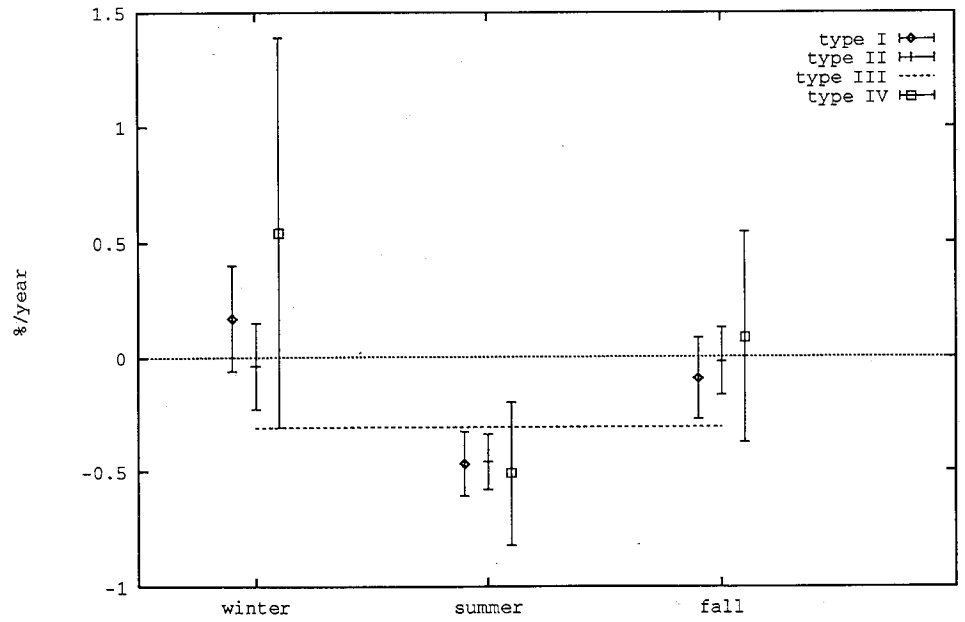

Figure 13b: Same as Figure 13a, for the period 1977–1990.

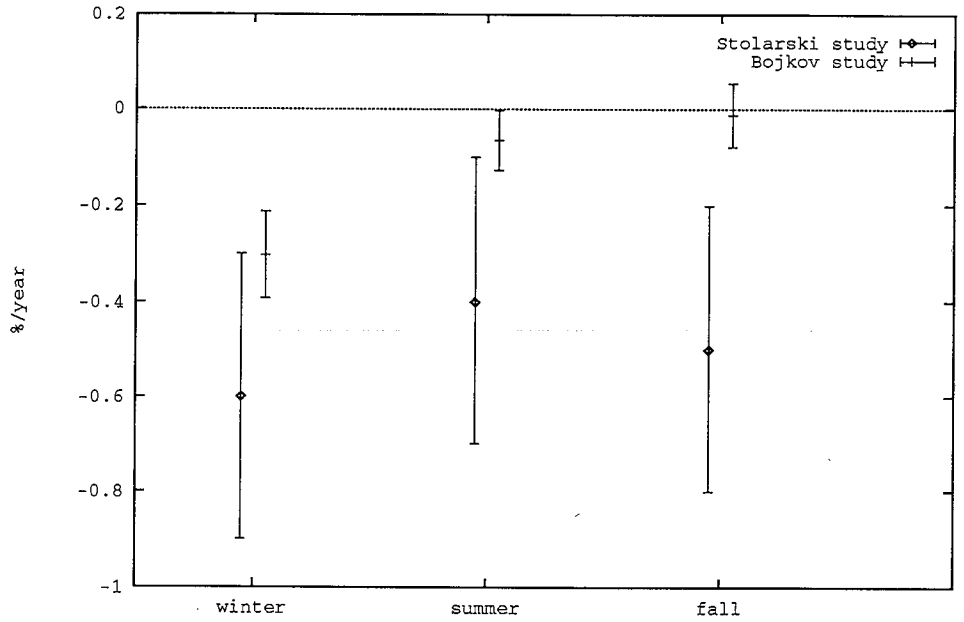

Figure 14: Linear trends from previous studies by Bojkov *et al.* (1990) and Stolarski *et al.* (1991). In the former study data from the Dobson network for the period 1958–1986 and latitude belt 53°–64°N was analyzed while the other used data from the TOMS satellite for 60°N and the period November 1978 to May 1990.

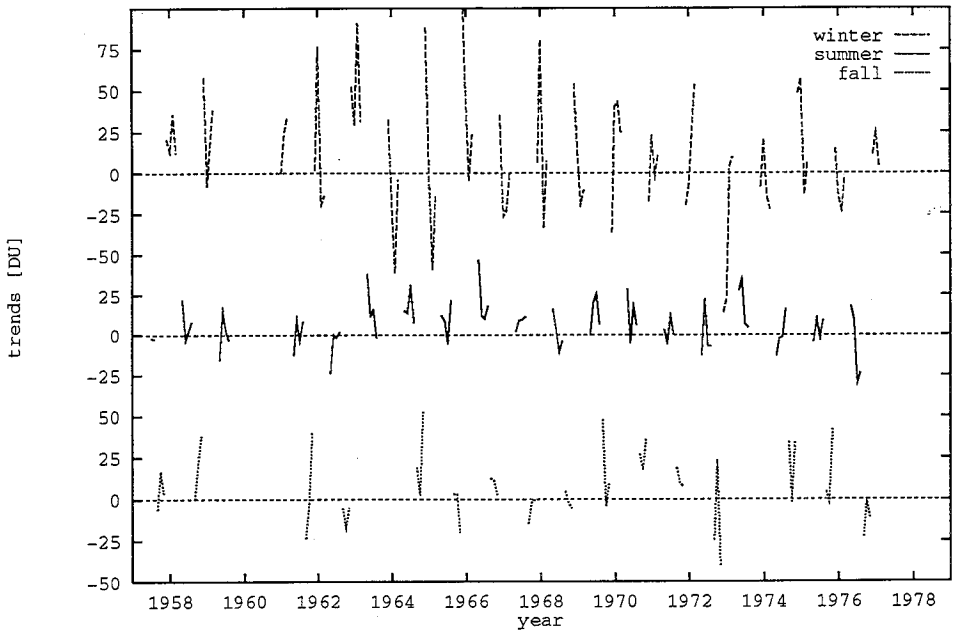

Figure 15a: Total ozone data (1957–1977) for each season after removal of modeled annual variations, QBO and solar effects.

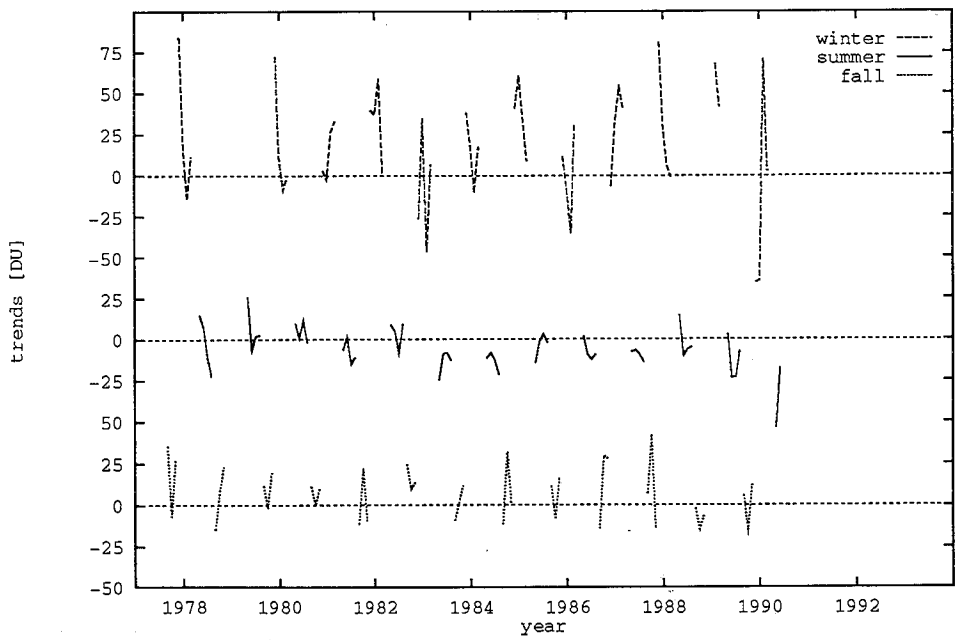

Figure 16b: Same as Figure 15a, except for the period 1977–1990.

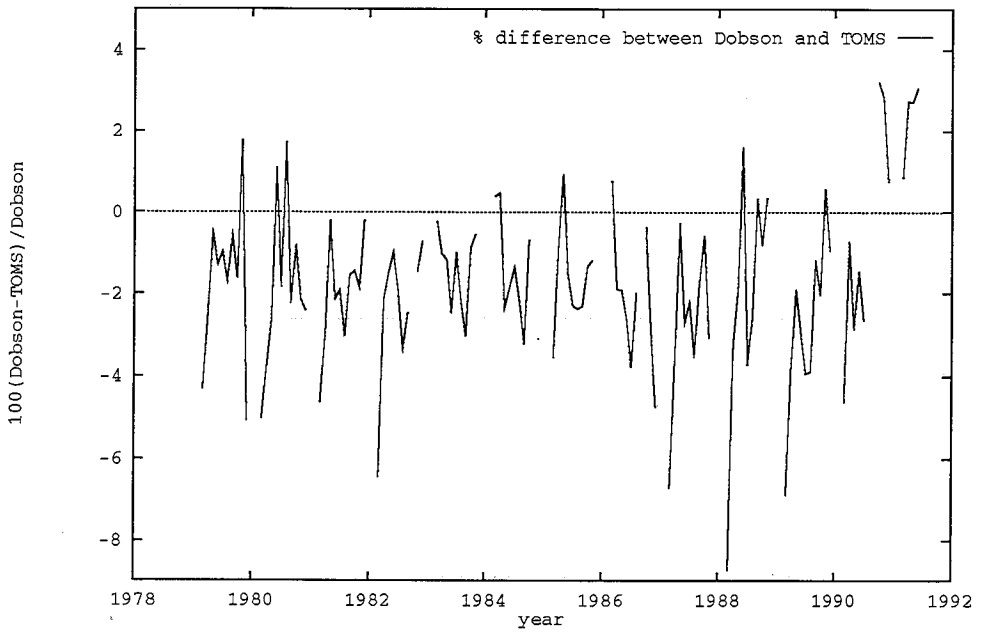

Figure 17a: Percentage difference between monthly means of the Dobson in Reykjavik and corresponding TOMS measurements, specially selected to represent Reykjavik. The TOMS data is version 6 and only months with at least 10 days of simultaneous Dobson and TOMS observations made at solar zenith angles not differing by more than 5° are shown. The data spans the period November 1978 to June 1991.

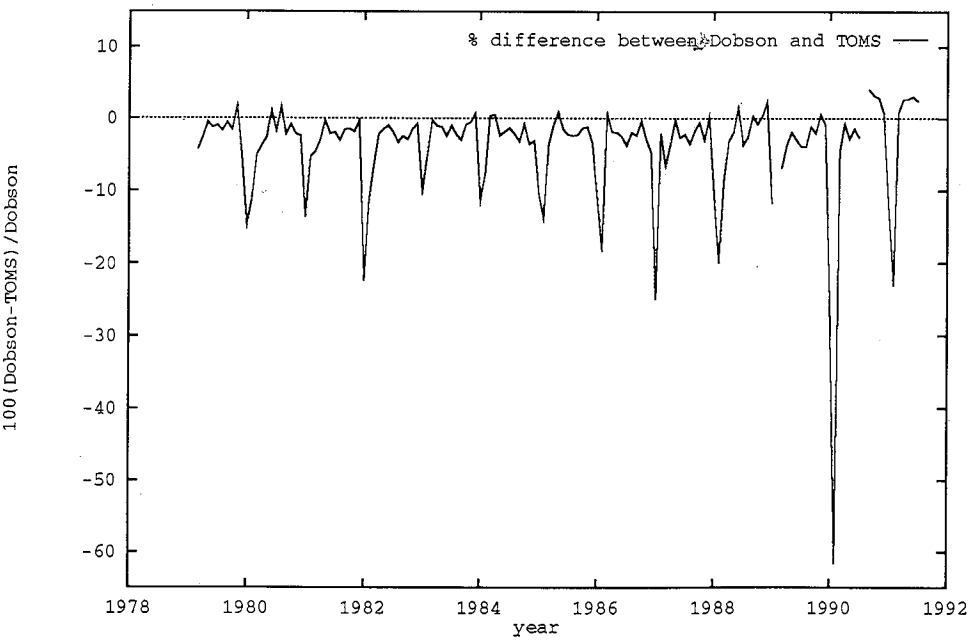

Figure 17b: Same as Figure 17a, except that all months are included.

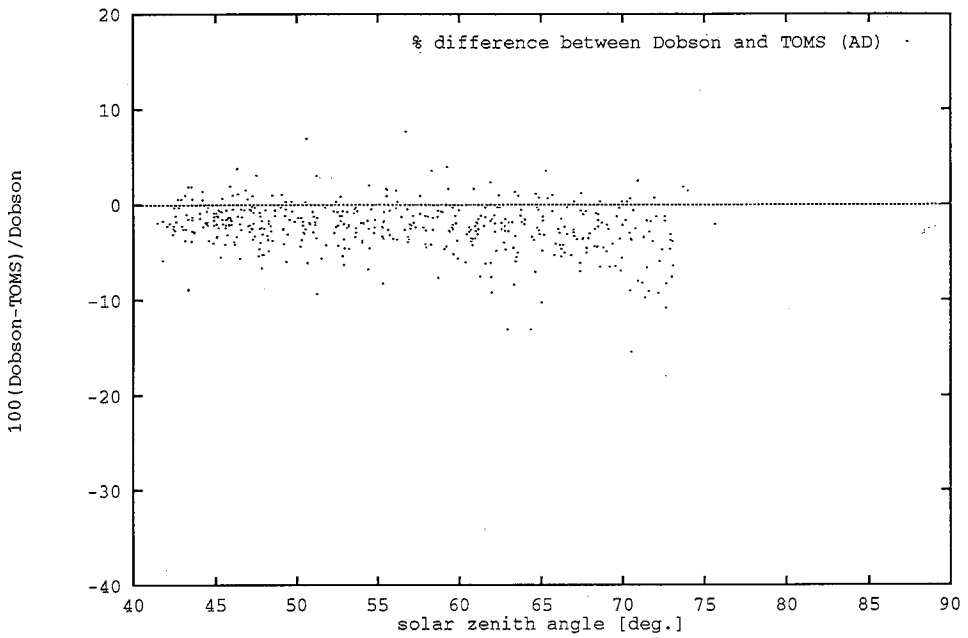

Figure 18a: Comparisons between Dobson and TOMS data for AD wavelength pairs as a function of solar zenith angle, calculated at times of satellite overpass.

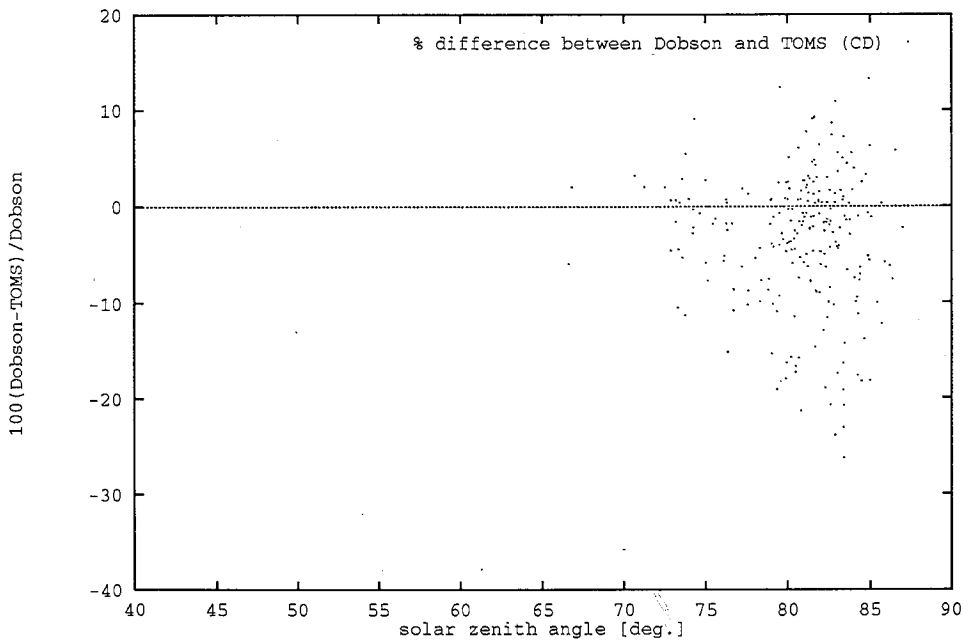

Figure 18b: Same as Figure 18a, except for CD wavelength pairs.

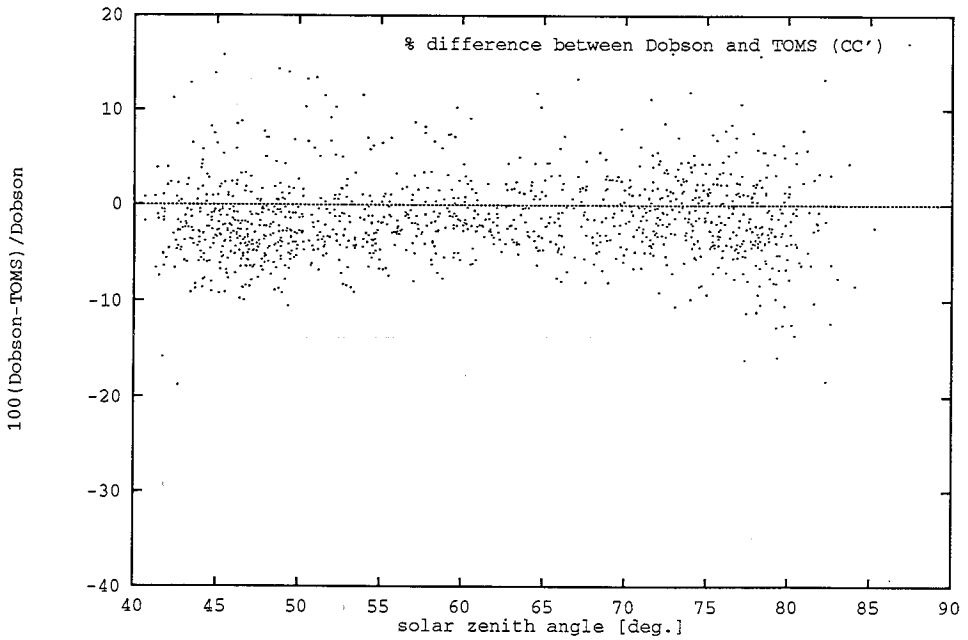

Figure 18c: Same as Figure 18a, except for CC′ wavelength pairs.

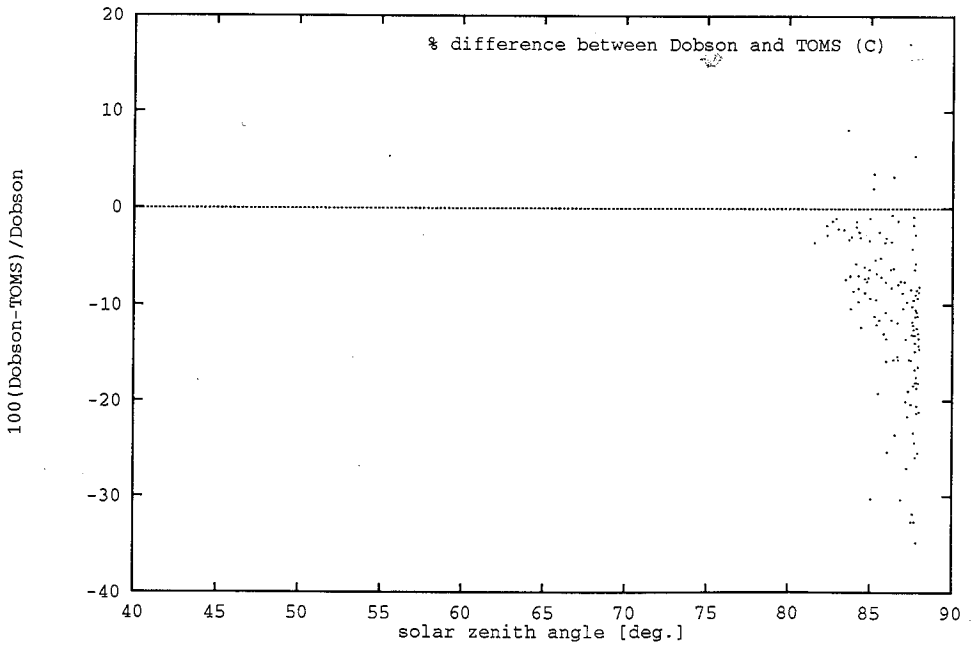

Figure 18d: Same as Figure 18a, except for C wavelength pair.

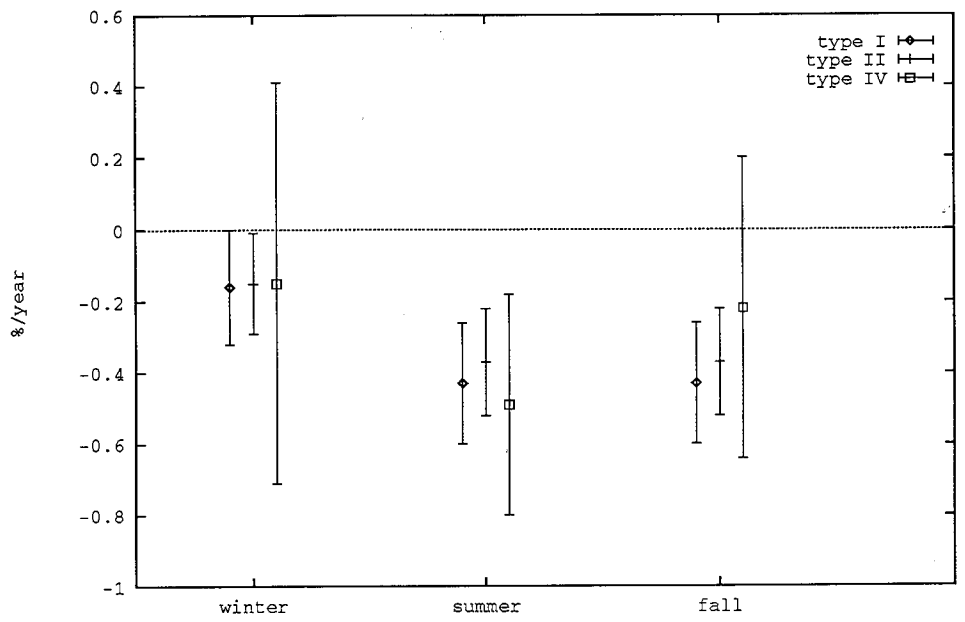

Figure 19: Linear trends deduced from the TOMS data using model types I, II and IV.

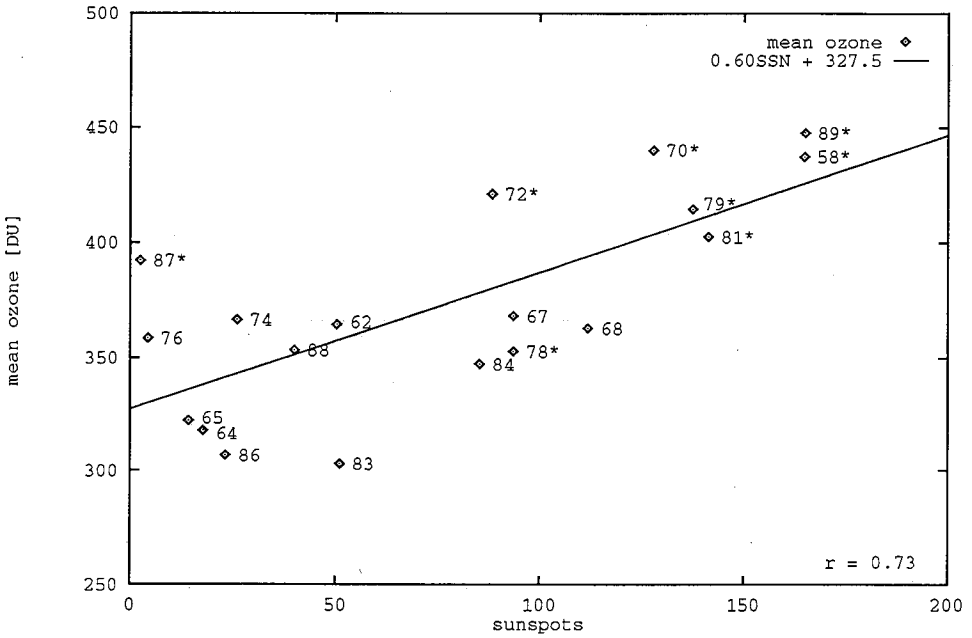

Figure 20a: Monthly averages of ozone as a function of sunspots in February for the west phase of the QBO. Years when major stratospheric warmings occur in February are marked with an asterisk. The linear relation between ozone and sunspots is $O_3 = (0.60 \pm 0.14)\mathrm{SSN} + 328 \pm 13$.

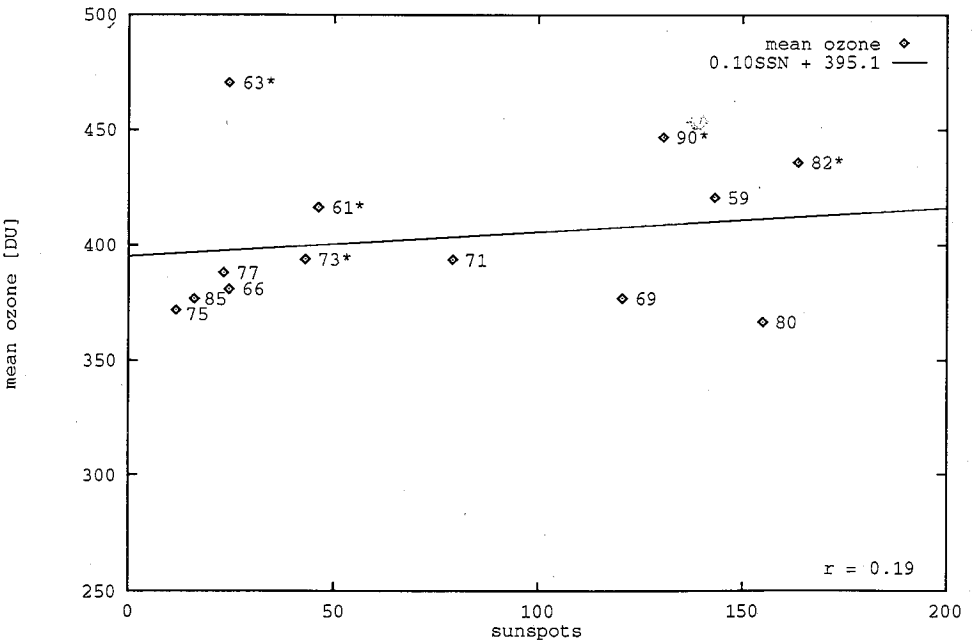

Figure 20b: Same as Figure 20a, except for the east phase of the QBO. The linear relation between ozone and sunspots is $O_3 = (0.11 \pm 0.16)\mathrm{SSN} + 395 \pm 15$.

References

[1] Anderson, J. G., D. W. Toohey, and W. H. Brune, *Free radicals within the antarctic vortex: The role of CFCs in antarctic ozone loss,* Science, **251**, 39–45, 1991.

[2] Angell, J. K., *Influence of equatorial QBO and SST on polar total ozone, and the 1990 antarctic ozone hole,* Geophys. Res. Lett., **17**, 1569–1572, 1990.

[3] Angell, J. K. and J. Korshover, *Global ozone variations: An update into 1976,* Mon. Wea. Rev., **106**, 725–737, 1978.

[4] Barthia, P. K., K. F. Klenk, C. K. Wong, and D. Gordon, *Intercomparison of the Nimbus 7 SBUV/TOMS total ozone data sets with Dobson and M83 results,* J. Geophys. Res., **89**, 5239–5247, 1984.

[5] Basher, R. E., *Review of the Dobson spectrophotometer and its accuracy,* Global Ozone Research and Monitoring Project, Report No. 13, World Meteorological Organization, Geneva, 1982.

[6] Bojkov, R. D., *Ozone variations in the northern polar region,* Meteorol. Atmos. Phys., **38**, 117–130, 1988.

[7] Bojkov, R. D., C. L. Mateer, and A. L. Hannson, *Comparison of ground-based and Total Ozone Mapping Spectrophotometer measurements used in assessing the performance of the Global Ozone Observing System,* J. Geophys. Res., **93**, 9525–9533, 1988.

[8] Bojkov, R., L. Bishop, W. J. Hill, G. C. Reinsel, and G. C. Tiao, *A statistical trend analysis of revised Dobson total ozone data over the northern hemisphere,* J. Geophys. Res., **95**, 9785–9807, 1990.

[9] Brasseur, G. and S. Solomon, *Aeronomy of the middle atmosphere,* Reidel Publishing Co., 2nd ed., 1986.

[10] Brasseur, G., M. H. Hickman, P. C. Simon, and A. DeRudder, *Ozone reduction in the 1980's: A model simulation of anthropogenic and solar perturbations,* Geophys. Res. Lett., **15**, 1361–1364, 1988.

[11] Brune, W. H., D. W. Toohey, J. G. Anderson, and K. R. Chan, *In situ observations of ClO in the arctic stratosphere: ER-2 aircraft results from 59°N to 80°N latitude,* Geophys. Res. Lett., **17**, 505–508, 1990.

[12] Chang, J. S., W. H. Duever, and D. J. Wuebbles, *The atmospheric nuclear tests of the 1950s and 1960s: A possible test of ozone depletion theories,* J. Geophys. Res., **84**, 1755–1765, 1979.

[13] Crutzen, P. and F. Arnold, *Nitric acid cloud formation in the cold antarctic stratosphere: A major cause for the springtime ozone hole,* Nature, **324**, 651–655, 1987.

[14] Dobson, G. M. B., *Observations of the amount of ozone in the Earth's atmosphere and its relation to other geophysical conditions,* Proc. Roy. Soc. London, Sec. A, **120**, 411, 1930.

[15] Dobson, G. M. B., *Exploring the atmosphere,* Clarendon Press, Oxford, 1968.

[16] Fahey, D. W., K. K. Kelly, G. V. Ferry, L. R. Poole, J. C. Wilson, D. M. Murphy, M. Loewenstein, and K. R. Chan, *In situ measurements of total reavtive nitrogen, total water, and aerosol in a polar stratospheric cloud in the Antarctic,* J. Geophys. Res., **94**, 11299–11316, 1989.

[17] Farman, J. C., B. G. Gardiner, and J. D. Shanklin, *Large losses of total ozone in Antarctica reveal seasonal ClO_x/NO_x interaction,* Nature, **315**, 207–210, 1985.

[18] Fiocco, G., D. Fua, M. Cacciani, P. D. Girolamo, and J. DeLuisi, *On the temperature dependence of polar stratospheric clouds,* Geophys. Res. Lett., **18**, 424–427, 1991.

[19] Garcia, R. R., S. Solomon, R. G. Roble, and D. W. Rusch, *A numerical study of the response of the middle atmosphere to the 11 year solar cycle,* Planet. Space Sci. **32**, 411–423, 1984.

[20] Garciá, R. R. and S. Solomon, *A possible relationship between interannual variability in antarctic ozone and the Quasi-Biennial Oscillation,* Geophys. Res. Lett., **14**, 848–851, 1987.

[21] Hamill, P., O. B. Toon, and R. P. Turco, *Characteristics of polar stratospheric clouds during the formation of the antarctic ozone hole,* Geophys. Res. Lett., **13**, 1288–1291, 1986.

[22] Hanson, D. and K. Mauersberger, *Laboratory studies of the nitric acid trihydrate: implications for the south polar stratosphere,* Geophys. Res. Lett., **15**, 855–858, 1988.

[23] Hasebe, F., *Interannual variation of global total ozone revealed from Nimbus 4 BUV and ground-based observatins,* J. Geophys. Res., **88**, 6819–6834, 1983.

[24] Hesse, B., *A comparison of total ozone data from satellite and ground-based observations at northern latitudes,* J. Geophys. Res., in press, 1992.

[25] Hofmann, D. J. and T. Deshler, *Evidence from balloon measurements for chemical depletion of stratospheric ozone in the arctic winter of 1989–90,* Nature, **349**, 300–305, 1991.

[26] Holton, J. T. and H.-C. Tan, *The influence of the equatorial quasi-biennial oscillation on the global circulation at 50mb,* J. Atmos. Sci., **37**, 2200–2208, 1980.

[27] Hood, L. L., *Coupled stratospheric ozone and temperature responses to short-term changes in solar ultraviolet flux: An analysis of Nimbus 7 SBUV and SAMS data,* J. Geophys. Res., **91**, 5264–5276, 1986.

[28] Keating, G. M., G. P. Brasseur, J. Y. Nicholson III, and A. DeRudder, *Detection of the response of ozone in the middle atmosphere to short-term solar ultraviolet variations,* Geophys. Res. Lett., **12**, 449–452, 1985.

[29] Koike, M., Y. Kondo, M. Hayashi, Y. Iwasaka, P. A. Newman, M. Helten, and P. Aimedieu, *Depletion of arctic ozone in the winter 1990,* Geophys. Res. Lett., **18**, 791–794, 1991.

[30] Labitzke, K., *Sunspots, the QBO, and the stratospheric temperature in the North Polar Region,* Geophys. Res. Lett., **14**, 535–537, 1987.

[31] Labitzke, K. and H. van Loon, *Associations between the 11-year solar cycle, the QBO and the atmosphere. Part I: The troposphere and stratosphere in the Northern Hemisphere in winter,* J. Atm. Terr. Phys., **50,3**, 197–206, 1988.

[32] Lait, L.R., M.R. Schoeberl, and P.A. Newman, Quasi-biennial modulation of the antarctic ozone depletion, J. Geophys. Res., 94, 11559-11571, 1989.

[33] London, J., *Radiative energy sources and sinks in the stratosphere and mesosphere,* pp 703-721, in: Nicolet, M. and Aikin, A. C. (eds.), *Proceedings of the NATO Advanced Study Institute on Atmospheric Ozone: Its variation and human influences,* U.S. Department of Transportation, Washington D.C., 1980.

[34] McCormick, M. P., A. M. Steele, P. Hamill, P. W. Chu, and T. J. Swissler, *Polar stratospheric clouds sightings by SAM II,* J. Atmos. Sci., **39**, 1387–1397, 1982.

[35] McElroy, M. B., R. I. Salawitch, S. C. Wofsy, and J. A. Logan, *Reduction of antarctic ozone due to synergistic interactions of chlorine and bromine,* Nature, **321**, 759–762, 1986.

[36] McPeters, R. D. and W. D. Komhyr, *Long-term changes in the total mapping spectrometer relative to World primary standard Dobson spectrometer 83,* J. Geophys. Res., **96**, 2987–2993, 1991.

[37] NASA/WMO Ozone Trends Panel, *Present state of knowledge of the upper atmosphere 1988: An assessment report,* NASA Ref. Publ. 1208, 1988.

[38] Newman, P. A., L. R. Lait, and M. R. Schoeberl, *The morphology and meteorology of Southern Hemisphere spring total ozone mini-holes,* Geophys. Res. Lett., **15**, 923–926, 1988.

[39] Newman, P. A., R. Stolarski, M. Schoeberl, L. R. Lait, and A. Krueger, *Total ozone during the 1988–89 northern hemisphere winter,* Geophys. Res. Lett., **17**, 317–320, 1990.

[40] Newman, P., R. Stolarski, M. Schoeberl, R. McPeters, and A. Krueger, *The 1990 antarctic ozone hole as observed by TOMS,* Geophys. Res. Lett., **18**, 661–664, 1991.

[41] Oltmans, S. J. and J. London, *The quasi-biennial oscillation in atmospheric ozone,* J. Geophys. Res., **87**, 8981–8989, 1982.

[42] Pommereau, J. P. and U. Schmidt, *CHEOPS III: An ozone research campaign in the arctic winter stratosphere: 1989/90,* Geophys. Res. Lett., **18**, 759–762, 1991.

[43] Poole, L. R., S. Solomon, M. P. McCormick, and M. C. Pitts, *The interannual variability of polar stratospheric clouds and related parameters in Antarctica during September and October,* Geophys. Res. Lett., **16**, 1157–1160, 1989.

[44] Reinsel, G. C., G. C. Tiao, A. J. Miller, D. J. Wuebbels, P. S. Connell, C. L. Mateer, and J. J. DeLuisi, *Statistical analysis of total ozone and stratospheric Umkehr Data for trends and solar cycle relationship,* J. Geophys. Res., **92**, 2201–2209, 1987.

[45] Rood, R. B., J. E. Nielsen, R. S. Stolarski, A. R. Douglass, J. A. Kaye, and J. Allen, *Episodic total ozone minima and associated effects on heterogeneous chemistry and lower startospheric transport,* in press, 1992.

[46] Schoeberl, M. R. and D. L. Hartmann, *The dynamics of the stratospheric polar vortex and its relation to springtime ozone depletions,* Science, **251**, 46–52, 1991.

[47] Seber, G. A. F. and C. J. Wild, *Nonlinear Regression,* John Wiley & Sons, 1989.

[48] Solomon, S., G. C. Reid, D. W. Rusch, and R. J. Thomas, *Mesospheric ozone depletion during the solar proton event of July 13, 1983, Part II. Comparison between theory and measurement,* Geophys. Res. Lett., **10**, 257–260, 1983.

[49] Solomon, S., R. R. Garcia, F. S. Rowland, and D. J. Wuebbles, *On the depletion of antarctic ozone,* Nature, **321**, 755–758, 1986.

[50] Solomon, S., *Progress towards a quantitative understanding of antarctic ozone depletion,* Nature, **347**, 347–354, 1990.

[51] Stolarski, R. S., P. Bloomfield, and R. D. McPeters, *Total ozone trends deduced from Nimbus 7 TOMS data,* Geophys. Res. Lett., **18**, 1015–1018, 1991.

[52] Turco, R., A. Plumb and E. Condon, *The Airborne Arctic Stratospheric Expedition: Prologue,* Geophys. Res. Lett., **17**, 313–316, 1990.

[53] van Loon, H., R. L. Jenne, and K. Labitzke, *Zonal harmonic standing waves,* J. Geophys. Res., **78**, 4463–4471, 1973.

[54] WMO, *Report of the International Ozone Trends Panel: 1988,* Global Ozone Research and Monitoring Project, Report No. 18, World Meteorological Organization, Geneva, 1990.

[55] Wuebbles, D. J., *A theoretical analysis of the post variations in global atmospheric composition and temperature structure,* Ph. D. Thesis, University of California, Livermore, 1983.

8 Appendix: Nonlinear Least Squares

Suppose that we have n observations $(\mathbf{x}_i, y_i), i = 1, 2, \ldots, n$ and that the relation between $\mathbf{x}_i$ and y_i is given by

$$\begin{aligned} y_i &= f(\mathbf{x}_i; \theta^*) + \epsilon_i \\ &= f_i(\theta^*) + \epsilon_i \end{aligned} \tag{10}$$

where the ϵ_i's are independent and normally distributed with variance σ_i^2 and θ^* is the vector of true model parameters. The least squares estimate of the model parameters, $\hat{\theta}$, minimizes the error sum of squares:

$$S(\theta) = \sum_{i=1}^{n} \left[\frac{y_i - f_i(\theta)}{\sigma_i} \right]^2. \tag{11}$$

We find the minimum by solving the set of equations:

$$\left. \frac{\partial S(\theta)}{\partial \theta_r} \right|_{\hat{\theta}} = 0 \quad (r = 1, 2, \ldots, p) \tag{12}$$

where p is the number of parameters in the nonlinear model. These equations can generally not be solved analytically so iterative methods are required. The simplest of these is the Gauss-Newton method, where we linearize the system, (12), by expanding it in a Taylor-series around $\hat{\theta}$ and retain only the linear part. This leads to an iteration scheme where $\theta^{(a+1)}$ is given by

$$\begin{aligned} \theta^{(a+1)} &= \theta^{(a)} + \delta^{(a)} \\ &= \theta^{(a)} + [\mathbf{F}^{(a)\prime}\mathbf{W}^{-1}\mathbf{F}^{(a)}]^{-1}\mathbf{F}^{(a)\prime}\mathbf{W}^{-1}[\mathbf{y} - \mathbf{f}(\theta^{(a)})] \end{aligned} \tag{13}$$

where $\mathbf{W}$ is the weight-matrix, $\mathbf{y} = (y_1, y_2, \ldots, y_n)'$, $\mathbf{f}(\theta) = (f_1(\theta), f_2(\theta), \ldots, f_n(\theta))'$, the prime denotes the transpose of a matrix and

$$\mathbf{F} = \frac{\partial \mathbf{f}(\theta)}{\partial \theta'} \tag{14}$$

so that $F_{ij} = \partial f_i(\theta)/\partial \theta_j$.

If the algorithm converges then $\delta^{(a)} \to \mathbf{0}$ as $a \to \infty$ and $\theta^{(a)}$ converges to a solution $\tilde{\theta}$ of

$$\mathbf{F}^{(a)\prime}\mathbf{W}^{-1}[\mathbf{y} - \mathbf{f}(\theta^{(a)})] = 0. \tag{15}$$

This method also gives an estimate of the asymptotic dispersion matrix of $\tilde{\theta}$,

$$\tilde{\mathbf{D}}[\tilde{\theta}] = \frac{S(\tilde{\theta})\,(\mathbf{F}'\mathbf{W}^{-1}\mathbf{F})^{-1}_{\tilde{\theta}}}{n - p}. \tag{16}$$

The variance of model parameter i is then estimated as, D_{ii}, the i-th diagonal element of $\tilde{\mathbf{D}}$.

In our nonlinear models we have used as a measure of convergence the relative-offset criterion described by Seber and Wild [1989, pp. 641-645]. The orthogonal projection of the residual vector, $\mathbf{r} = \mathbf{y} - \mathbf{f}$, onto the column space of $\mathbf{F}$ is given by

$$\mathbf{r}_T = \mathbf{F}(\mathbf{F}'\mathbf{F})^{-1}\mathbf{F}'\mathbf{r}. \tag{17}$$

At the minimum of $S(\theta)$, $\hat{\mathbf{r}}_T \equiv \mathbf{r}(\hat{\theta}) = \mathbf{0}$. Convergence of the iteration is then declared if $\mathbf{r}_T^{(a)}$ is small in some sense (note that $\mathbf{r}_T^{(a)}$ is the orthogonal projection of the residual vector $\mathbf{r}^{(a)} = \mathbf{y} - \mathbf{f}^{(a)}$ onto the tangent plane at $\theta^{(a)}$). We have used the criterion suggested by Seber and Wild (page 642, equation 14.71) and stop the iteration when

$$P^{(a)} = \frac{\| \mathbf{r}_T^{(a)} \|}{\rho} < \tau, \tag{18}$$

where

$$\rho = \left(\frac{pS(\theta^{(a)})}{n-p} \right)^{1/2}. \tag{19}$$

$P^{(a)}$ is called the relative offset at $\theta^{(a)}$. We take $\tau = 0.001$, the convergence criterion is then usually reached after 5–10 iterations of equation (13).